Global stability of multi-group SAIRS epidemic models

Received: 8 July 2022 | Revised: 8 April 2023 | Accepted: 8 April 2023

DOI: 10.1002/mma.9303

RESEARCH ARTICLE

WILEY

Global stability of multi-group SAIRS epidemic models

Stefania Ottaviano[1,2] | **Mattia Sensi**[3,4] | **Sara Sottile**[5]

[1]Department of Mathematics "Tullio Levi Civita", University of Padua, Padova, Italy

[2]Department of Civil, Environmental and Mechanical Engineering, University of Trento, Trento, Italy

[3]MathNeuro Team, Inria at Université Côte d'Azur, Biot, France

[4]Politecnico di Torino, Torino, Italy

[5]Department of Mathematics, University of Trento, Trento, Italy

Correspondence
Mattia Sensi, MathNeuro Team, Inria at Université Côte d'Azur, 2004 Rte des Lucioles, 06410 Biot, France.
Email: mattia.sensi@polito.it

Communicated by: E. Venturino

Funding information
Italian Ministry for University and Research (MUR), Grant/Award Number: 2020JLWP23; University of Trento, Grant/Award Number: 40900013

We study a multi-group SAIRS-type epidemic model with vaccination. The role of asymptomatic and symptomatic infectious individuals is explicitly considered in the transmission pattern of the disease among the groups in which the population is divided. This is a natural extension of the homogeneous mixing SAIRS model with vaccination studied in Ottaviano et. al (2021) to a network of communities. We provide a global stability analysis for the model. We determine the value of the basic reproduction number $\mathcal{R}_0$ and prove that the disease-free equilibrium is globally asymptotically stable if $\mathcal{R}_0 < 1$. In the case of the SAIRS model without vaccination, we prove the global asymptotic stability of the disease-free equilibrium also when $\mathcal{R}_0 = 1$. Moreover, if $\mathcal{R}_0 > 1$, the disease-free equilibrium is unstable and a unique endemic equilibrium exists. First, we investigate the local asymptotic stability of the endemic equilibrium and subsequently its global stability, for two variations of the original model. Last, we provide numerical simulations to compare the epidemic spreading on different networks topologies.

KEYWORDS

basic reproduction number, global asymptotic stability, graph-theoretic method, Lyapunov functions, multi-group models, susceptible–asymptomatic infected–symptomatic infected–recovered–susceptible, vaccination

MSC CLASSIFICATION

34A34, 34D20, 34D23, 37N25, 92D30

1 | INTRODUCTION

One of the most common assumptions in classic population models is the homogeneity of interactions between individuals, which then happen completely at random. While such an assumption significantly simplifies the analysis of the models, it can be beneficial to renounce it and to formulate models with more realistic interactions. Heterogeneity in the interactions among the population can depend on many factors. The most common division regards the geographical distinction and the membership to different communities, cities or countries, in which the same infectious disease can have a different behavior based on the group under study.

The division in groups can also depend on the specific disease under study. For example, individuals can be divided into age groups to study children's diseases, such as measles, mumps, or rubella, or can be differentiated by the number of sexual partners for sexually transmitted infections.

Multi-group models can also be useful to study disease transmitted via vectors or multiple hosts, such as Malaria or West Nile virus.

The concept of equitable partitions has been used to study networks partitioned into local communities with some regularities in their structure, in the case of SIS and SIRS models [1–3], by means of the N-intertwined mean-field approximation [4]. In the aforementioned works, the macroscopic structure of hierarchical networks is described by a quotient graph and the stability of the endemic equilibrium can be investigated by a lower dimensional system with respect to the starting one.

Several authors proposed multi-group models to describe the transmission behavior between different communities or cities; see, for example, previous studies [5–7]. In this paper, we assume that each individual interacts within a network of relationships, due to, for example, different social or spatial patterns; individuals are hence divided into groups, which are not isolated from one another.

As in the homogeneous mixing case, the stability analysis of the equilibrium points of the system under investigation allows to understand its long-term behavior and, hence, to obtain some insight into how the prevalence of an endemic disease depends on the parameters of the model [8] and, in this case, on the network topology. However, the problem of existence and global stability, especially for the endemic equilibrium, is often mathematical challenging; unfortunately, for many complex multi-group models, it remains an open question or requires cumbersome conditions [9]. In this framework, Guo et al. [10, 11] and Li and Shuai [12] developed a graph-theoretic method to find Lyapunov functions for some multi-group epidemic models which has recently allowed to obtain various results on the global dynamics of SIRS-type models [13, 14] and SEIRS-type models [15].

In this paper, we present a multi-group model, as extension of the SAIRS-type model proposed in Ottaviano et al. [16], where the role of asymptomatic and symptomatic infectious individuals in the disease transmission has been explicitly considered. Asymptomatic cases often remain unidentified and possibly have more contacts than symptomatic individuals, allowing the virus to circulate widely in the population [17–20]. The so-called "silent spreaders" are playing a significant role even in the current Covid-19 pandemic and numerous recent papers have considered their contribution in the virus transmission (see, e.g., previous studies [21–25]). However, this contribution has proved relevant also for other communicable diseases, such as influenza, cholera, and shigella [26–29].

Although models incorporating asymptomatic individuals already exist in the literature, they have not been analytically investigated as thoroughly as more famous compartmental models. Since these types of models have been receiving much more attention lately, we believe they deserve a deeper understanding from a theoretical point of view. Thus, we aim to partially fill this gap and provide a stability analysis of the multi-group system under investigation.

In our model, we denote with S_i, A_i, I_i, and R_i, $i = 1, \dots, n$, the fraction of Susceptible, Asymptomatic infected, symptomatic Infected, and Recovered individuals, respectively, in the ith group, such that $S_i + A_i + I_i + R_i = 1$. We remark that, from here on, we will use the terms community and group interchangeably.

The disease can be transmitted by individuals in the classes A_i and I_i, within their group, to the susceptible S_i, with transmission rate β_{ii}^A and β_{ii}^I, respectively, and between different groups: For example, individuals A_j and I_j, belonging to the jth community, may infect susceptible individuals S_i of group i with transmission rate β_{ij}^A and β_{ij}^I, respectively. From the asymptomatic compartment, an individual can either progress to the class of symptomatic infectious or recover without ever developing symptoms. We assume that the average time of the symptoms developing, denoted by $1/\alpha$, and the recovery rates from both the infectious compartments, δ_A and δ_I, do not depend on the community of origin, that is, these parameters depend only on the disease. Furthermore, the average time to return to the susceptible state, $1/\gamma$, only depends on the specific disease under study, and not on the community to which an individual belongs. The remaining parameters of the model depend on the community's membership. First, the proportion of susceptible individuals who receive the vaccine might be different for each group; we denote with ν_i, $i = 1, \dots, n$, the proportion of susceptible in the ith group who receive a vaccine-induced temporary immunity. Moreover, μ_i, $i = 1, \dots, n$ represent both the birth rates and the natural death rates in community i. Finally, individuals of different communities may have contacts each other, by direct transport, but they never permanently move to another community. Therefore, the total population in each group may only change through births and natural deaths; we do not distinguish between natural deaths and disease-related deaths.

1.1 | Outline

The paper is organized as follows. In Section 2, we present the system of equations for the multi-group SAIRS model with vaccination, providing its positive invariant set. In Section 3, we determine the basic reproduction number $\mathcal{R}_0$ and prove that the disease-free equilibrium (DFE) is globally asymptotically stable (GAS) if $\mathcal{R}_0 < 1$ and unstable if $\mathcal{R}_0 > 1$.

Moreover, we prove the GAS of the DFE also in the case $\mathcal{R}_0 = 1$, for the model in which no vaccination is administered to the susceptible individuals. In Section 4, we prove the existence and uniqueness of an endemic equilibrium (EE) by a fixed point argument, as in Thieme [8], since there is no explicit expression for $\mathcal{R}_0$. In Section 4.1, we provide sufficient conditions for the local asymptotic stability of the EE. In Section 5, we discuss the uniform persistence of the disease and we investigate the global asymptotic stability of the EE for two variations of the original model under study. Precisely, in Theorem 14, we study the global stability of the SAIR model (i.e., $\gamma = 0$), and we prove that the EE is GAS if $\mathcal{R}_0 > 1$. In Section 5.2, we establish sufficient conditions for the GAS of the EE for the SAIRS model (i.e., $\gamma \neq 0$) with vaccination, under the restriction that asymptomatic and symptomatic individuals have the same average recovery period, that is, $\delta_A = \delta_I$. The problem of the global stability of the EE in the most general case, that is, $\delta_A \neq \delta_I$, remains open. In Section 6, we provide some numerical simulations in which we simulate the evolution of the epidemics in four different structures of community networks.

2 | THE MODEL

The system of ODEs that describes the evolution of the disease in the ith community is the following:

$$\begin{aligned}
\frac{dS_i(t)}{dt} &= \mu_i - \sum_{j=1}^{n} \left(\beta_{ij}^A A_j(t) + \beta_{ij}^I I_j(t)\right) S_i(t) - (\mu_i + \nu_i) S_i(t) + \gamma R_i(t),\\
\frac{dA_i(t)}{dt} &= \sum_{j=1}^{n} \left(\beta_{ij}^A A_j(t) + \beta_{ij}^I I_j(t)\right) S_i(t) - (\alpha + \delta_A + \mu_i) A_i(t),\\
\frac{dI_i(t)}{dt} &= \alpha A_i(t) - (\delta_I + \mu_i) I_i(t),\\
\frac{dR_i(t)}{dt} &= \delta_A A_i(t) + \delta_I I_i(t) + \nu_i S_i(t) - (\gamma + \mu_i) R_i(t),\ i = 1, \dots, n,
\end{aligned} \tag{1}$$

with initial condition $(S_1(0), A_1(0), I_1(0), R_1(0), \dots, S_n(0), A_n(0), I_n(0), R_n(0))$ belonging to the set

$$\bar{\Gamma} = \{(S_1, A_1, I_1, R_1, \dots, S_n, A_n, I_n, R_n) \in \mathbb{R}_+^{4n} | S_i + A_i + I_i + R_i = 1, i = 1, \dots, n\}, \tag{2}$$

where $\mathbb{R}_+^{4n}$ indicates the non-negative orthant of $\mathbb{R}^{4n}$. The flow diagram representing the interaction among two groups of system (1), as well as their internal dynamics, is given in Figure 1.

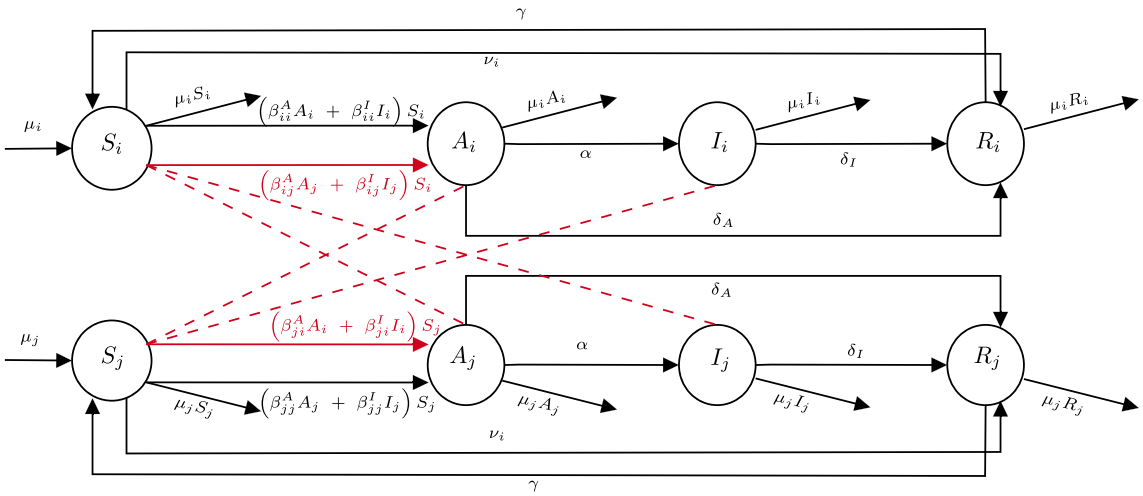

FIGURE 1 Flow diagram for system (1), depicting the interaction between communities i and j, as well as their internal dynamics. The solid lines represent internal dynamics within each group, whereas the dashed lines represent the inter-group influence of infected individuals. [Colour figure can be viewed at wileyonlinelibrary.com]

Assuming initial conditions in $\bar{\Gamma}$, $S_i(t) + A_i(t) + I_i(t) + R_i(t) = 1$, for all $t \geq 0$ and $i = 1, \dots, n$; hence, system (1) is equivalent to the following $3n$-dimensional dynamical system:

$$\begin{aligned}
\frac{dS_i(t)}{dt} &= \mu_i - \sum_{j=1}^{n} \left(\beta_{ij}^A A_j(t) + \beta_{ij}^I I_j(t)\right) S_i(t) - (\mu_i + \nu_i + \gamma) S_i(t) + \gamma(1 - A_i(t) - I_i(t)), \\
\frac{dA_i(t)}{dt} &= \sum_{j=1}^{n} \left(\beta_{ij}^A A_j(t) + \beta_{ij}^I I_j(t)\right) S_i(t) - (\alpha + \delta_A + \mu_i) A_i(t), \\
\frac{dI_i(t)}{dt} &= \alpha A_i(t) - (\delta_I + \mu_i) I_i(t), \quad i = 1, \dots, n,
\end{aligned} \tag{3}$$

with initial condition $(S_1(0), A_1(0), I_1(0), \dots, S_n(0), A_n(0), I_n(0))$ belonging to the set

$$\Gamma = \left\{(S_1, A_1, I_1, \dots, S_n, A_n, I_n) \in \mathbb{R}_+^{3n} | S_i + A_i + I_i \leq 1, i = 1, \dots, n\right\}.$$

System (3) can be written in vector notation as

$$\frac{dx(t)}{dt} = f(x(t)), \tag{4}$$

where $x(t) = (S_1(t), A_1(t), I_1(t), \dots, S_n(t), A_n(t), I_n(t))$ and $f(x(t)) = (f_1(x(t)), f_2(x(t)), \dots, f_{3n}(x(t)))$ is defined according to (3).

We make the following assumptions:

Assumption 1.

- The matrices $[\beta_{ij}^A]_{i,j=1,\dots,n}$ and $[\beta_{ij}^I]_{i,j=1,\dots,n}$ are irreducible. This means that every pair of communities is connected by a path.
- $\beta_{ii}^A \neq 0$, $\beta_{ii}^I \neq 0$, $i = 1, \dots, n$. This means that infection can spread within each community.

Theorem 1. *Γ is positively invariant for system (3). That is, for all initial values $x(0) \in \Gamma$, the solution $x(t)$ of (3) will remain in Γ for all $t > 0$.*

Proof. Let us consider the boundary $\partial\Gamma$, as in Ottaviano et al. [16, Th. 1]. It consists of the following hyperplanes:

$$\begin{aligned}
H_{1,i} &= \{(S_1, A_1, I_1, \dots, S_n, A_n, I_n) \in \Gamma \mid S_i = 0\}, \\
H_{2,i} &= \{(S_1, A_1, I_1, \dots, S_n, A_n, I_n) \in \Gamma \mid A_i = 0\}, \\
H_{3,i} &= \{(S_1, A_1, I_1, \dots, S_n, A_n, I_n) \in \Gamma \mid I_i = 0\}, \\
H_{4,i} &= \{(S_1, A_1, I_1, \dots, S_n, A_n, I_n) \in \Gamma \mid S_i + A_i + I_i = 1\}, \qquad i = 1, \dots, n.
\end{aligned}$$

Let us consider $H_{k,1}$, $k = 1, 2, 3, 4$. The outward normal vectors of $H_{1,1}$, $H_{2,1}$, $H_{3,1}$, and $H_{4,1}$ are, respectively,

$$\begin{aligned}
\eta_{1,1} &= (-1, 0, 0, \dots, 0, 0, 0), \qquad \eta_{2,1} = (0, -1, 0, \dots, 0, 0, 0), \\
\eta_{3,1} &= (0, 0, -1, \dots, 0, 0, 0), \qquad \eta_{4,1} = (1, 1, 1, \dots, 0, 0, 0).
\end{aligned}$$

Let $x \in H_{k,1}$, $k = 1, \dots, 4$, and consider the following cases:

Case 1: $S_1 = 0$. Then, since $A_1 + I_1 \leq 1$,

$$\langle f(x), \eta_{1,1} \rangle = -\mu_1 - \gamma(1 - A_1 - I_1) \leq 0.$$

Case 2: $A_1 = 0$. Then, since $S_1 \geq 0, A_i \geq 0, I_i \geq 0, i = 2, \dots, n$,

$$\langle f(x), \eta_{2,1} \rangle = -\underbrace{\left(\sum_{j=2}^{n} \beta_{ij}^{A} A_j + \sum_{j=1}^{n} \beta_{ij}^{I} I_j \right)}_{\geq 0} S_1 \leq 0.$$

Case 3: $I_1 = 0$. Then, since $A_1 \geq 0$,

$$\langle f(x), \eta_{3,1} \rangle = -\alpha A_1 \leq 0.$$

Case 4: $S_1 + A_1 + I_1 = 1$. Then, since $S_1 \geq 0, A_1 \geq 0, I_1 \geq 0$,

$$\langle f(x), \eta_{4,1} \rangle = -\nu_1 S_1 - \delta_A A_1 - \delta_I I_1 \leq 0.$$

The proof for the hyperplanes $H_{k,i}$, $k = 1, \dots, 4$ and $i = 2, \dots, n$ is analogous. □

3 | DISEASE ELIMINATION

System (3) always admits a DFE, whose expression is

$$x_0 = \left(S_{0,1}, A_{0,1}, I_{0,1}, \dots, S_{0,n}, A_{0,n}, I_{0,n} \right),$$

where

$$S_{0,i} = \frac{\gamma + \mu_i}{\gamma + \mu_i + \nu_i}, \quad A_{0,i} = I_{0,i} = 0, \quad i = 1, \dots, n. \tag{5}$$

Note that, in general, $S_{0,i} \neq S_{0,j}$ if $i \neq j$.

Lemma 2. *Consider the matrix*

$$M_1 = \left(\left(\beta_{ij}^{A} + \frac{\alpha \beta_{ij}^{I}}{\delta_I + \mu_i} \right) \frac{S_{0,i}}{\alpha + \delta_A + \mu_i} \right)_{i,j=1,\dots,n}.$$

The basic reproduction number $\mathcal{R}_0$ of (3) is

$$\mathcal{R}_0 = \rho(M_1) = \rho \left(\left(\left(\beta_{ij}^{A} + \frac{\alpha \beta_{ij}^{I}}{(\delta_I + \mu_i)} \right) \frac{\gamma + \mu_i}{(\gamma + \mu_i + \nu_i)(\alpha + \delta_A + \mu_i)} \right)_{i,j=1,\dots,n} \right), \tag{6}$$

where $\rho(M_1)$ is the spectral radius of the matrix M_1.

Proof. We shall use the next generation matrix method [30] to find $\mathcal{R}_0$. System (3) has $2n$ disease compartments, namely A_i and I_i, $i = 1, \dots, n$. Rearranging the order of the equations such that the disease compartments can be written as $x = (A_1, \dots, A_n, I_1, \dots, I_n)^T$, we can rewrite the corresponding ODEs as

$$\begin{aligned} \frac{dA_i(t)}{dt} &= \mathcal{F}_{1_i}(S_i(t), A_i(t), I_i(t)) - \mathcal{V}_{1,i}(S_i(t), A_i(t), I_i(t)), \\ \frac{dI_i(t)}{dt} &= \mathcal{F}_{2,i}(S_i(t), A_i(t), I_i(t)) - \mathcal{V}_{2,i}(S_i(t), A_i(t), I_i(t)), \end{aligned}$$

where

$$\mathcal{F}_{1,i} = \sum_{i=1}^{n} \left(\beta_{ij}^{A} A_j(t) + \beta_{ij}^{I} I_j(t) \right) S_i(t), \qquad \mathcal{V}_{1,i} = (\alpha + \delta_A + \mu_i) A_i(t),$$

$$\mathcal{F}_{2,i} = 0, \qquad \mathcal{V}_{2,i} = -\alpha A_i(t) + (\delta_I + \mu_i) I_i(t).$$

Thus, we obtain

$$F = \begin{pmatrix} \left(\frac{\partial \mathcal{F}_{1,i}}{\partial A_j}(x_0)\right)_{i,j=1,\dots,n} & \left(\frac{\partial \mathcal{F}_{1,i}}{\partial I_j}(x_0)\right)_{i,j=1,\dots,n} \\ \left(\frac{\partial \mathcal{F}_{2,i}}{\partial A_j}(x_0)\right)_{i,j=1,\dots,n} & \left(\frac{\partial \mathcal{F}_{2,i}}{\partial I_j}(x_0)\right)_{i,j=1,\dots,n} \end{pmatrix}, \tag{7}$$

$$V = \begin{pmatrix} \left(\frac{\partial \mathcal{V}_{1,i}}{\partial A_j}(x_0)\right)_{i,j=1,\dots,n} & \left(\frac{\partial \mathcal{V}_{1,i}}{\partial I_j}(x_0)\right)_{i,j=1,\dots,n} \\ \left(\frac{\partial \mathcal{V}_{2,i}}{\partial A_j}(x_0)\right)_{i,j=1,\dots,n} & \left(\frac{\partial \mathcal{V}_{2,i}}{\partial I_j}(x_0)\right)_{i,j=1,\dots,n} \end{pmatrix}, \tag{8}$$

which can be written in matrix notation

$$F = \begin{pmatrix} \tilde{B}^A & \tilde{B}^I \\ 0 & 0 \end{pmatrix} \text{ and } V = \begin{pmatrix} (\alpha+\delta_A)\mathbb{I}+\mu & 0 \\ -\alpha\mathbb{I} & \delta_I\mathbb{I}+\mu \end{pmatrix},$$

where $(\tilde{B}^A)_{ij} = \beta^A_{ij} S_{0,i}$, $(\tilde{B}^I)_{ij} = \beta^I_{ij} S_{0,i}$, $\mu = \mathrm{diag}(\mu_1, \dots, \mu_n)$, and 0 and $\mathbb{I}$ are the zero matrix and the identity matrix of order n, respectively. Since V is a block lower triangular matrix, its inverse is the $2n \times 2n$ block matrix:

$$V^{-1} = \begin{pmatrix} \mathrm{diag}\left(\frac{1}{\alpha+\delta_A+\mu_i}\right)_{i=1,\dots,n} & 0 \\ \mathrm{diag}\left(\frac{\alpha}{(\alpha+\delta_A+\mu_i)(\delta_I+\mu_i)}\right)_{i=1,\dots,n} & \mathrm{diag}\left(\frac{1}{\delta_I+\mu_i}\right)_{i=1,\dots,n} \end{pmatrix}.$$

The next generation matrix is defined as $M := FV^{-1}$. By direct calculation, we obtain

$$M = \begin{pmatrix} \left(\left(\frac{\beta^A_{ij}}{\alpha+\delta_A+\mu_i} + \frac{\alpha\beta^I_{ij}}{(\alpha+\delta_A+\mu_i)(\delta_I+\mu_i)}\right) S_{0,i}\right)_{i,j=1,\dots,n} & \left(\frac{\beta^I_{ij} S_{0,i}}{\delta_I+\mu_i}\right)_{i,j=1,\dots,n} \\ 0 & 0 \end{pmatrix}. \tag{9}$$

The basic reproduction number $\mathcal{R}_0$ is defined as the spectral radius of M, denoted by $\rho(M)$, that is, $\rho(M) = \max\{\rho(M_1), 0\}$, where

$$M_1 = \left(\left(\beta^A_{ij} + \frac{\alpha\beta^I_{ij}}{\delta_I+\mu_i}\right)\frac{S_{0,i}}{\alpha+\delta_A+\mu_i}\right)_{i,j=1,\dots,n}. \tag{10}$$

As a direct consequence of the Perron–Frobenius theorem [31], $\rho(M_1) > 0$. This proves our claim. □

In the following, we present some results to prove the global asymptotic stability of the DFE x_0.

Recall that a matrix M is called *non-negative* if each entry is non-negative; we simply write $M \geq 0$ to indicate this. We use the following results from van den Driessche and Watmough [32]:

Lemma 3 (van den Driessche and Watmough [32, Lemma 2])**.** *If F is non-negative and V is a non-singular M-matrix, then $\mathcal{R}_0 = \rho(FV^{-1}) < 1$ if and only if all eigenvalues of $(F - V)$ have negative real parts.*

Note that the matrices F and V defined in Lemma 2 satisfy the hypotheses of Lemma 3; thus, the following result holds:

Theorem 4. *The DFE of (3) is locally asymptotically stable if $\mathcal{R}_0 < 1$ and unstable if $\mathcal{R}_0 > 1$.*

Proof. See van den Driessche and Watmough [32, Theorem 1]. □

Theorem 5. *The DFE x_0 of (3) is GAS in Γ if $\mathcal{R}_0 < 1$.*

Proof. Let $x(t) = (S_1(t), \dots, S_n(t), A_1(t), \dots, A_n(t), I_1(t) \dots, I_n(t))$ be the solutions of system (3) with initial condition $x(0) \in \Gamma$, in which we have rearranged the order of the equations. In view of Theorem 4, it is sufficient to prove that for all $i = 1, \dots, n$,

$$\lim_{t\to\infty} S_i(t) = S_{0,i}, \qquad \lim_{t\to\infty} A_i(t) = 0, \qquad \text{and} \qquad \lim_{t\to\infty} I_i(t) = 0,$$

with $S_{0,i}$ as in (5). From the first n equations of (3), it follows that

$$\frac{dS_i(t)}{dt} \le \mu_i + \gamma - (\mu_i + \nu_i + \gamma)S_i(t), \quad i = 1, \dots, n.$$

Thus, $S_{0,i}$ is a global asymptotically stable equilibrium for the comparison equation

$$\frac{dz_i(t)}{dt} = \mu_i + \gamma - (\mu_i + \nu_i + \gamma)z_i(t), \quad i = 1, \dots, n.$$

Then, for any $\varepsilon > 0$, there exists $\bar{t}_i > 0$, such that for all $t \ge \bar{t}_i$, it holds

$$S_i(t) \le S_{0,i} + \varepsilon, \tag{11}$$

hence,

$$\limsup_{t\to\infty} S_i(t) \le S_{0,i}, \qquad i = 1, \dots, n. \tag{12}$$

Let $\bar{t} = \max\{t_1, \dots, t_n\}$, then for all $t \ge \bar{t}$, from (11) and the remaining $2n$ equations of (3), it follows that

$$\begin{aligned}
\frac{dA_i(t)}{dt} &\le \sum_{j=1}^{n} \left(\beta_{ij}^A A_j(t) + \beta_{ij}^I I_i(t)\right)(S_{0,i} + \varepsilon) - (\alpha + \delta_A + \mu_i)A_i(t), \qquad i = 1, \dots, n,\\
\frac{dI_i(t)}{dt} &= \alpha A_i(t) - (\delta_I + \mu_i)I_i(t), \qquad i = 1, \dots, n.
\end{aligned}$$

Let us now consider the comparison system

$$\begin{aligned}
\frac{dv_i(t)}{dt} &= \sum_{j=1}^{n} \left(\beta_{ij}^A v_j(t) + \beta_{ij}^I u_i(t)\right)(S_{0,i} + \varepsilon) - (\alpha + \delta_A + \mu_i)v_i(t),\\
\frac{du_i(t)}{dt} &= \alpha v_i(t) - (\delta_I + \mu)u_i(t), \qquad v_i(\bar{t}) = A_i(\bar{t}),\ u_i(\bar{t}) = I_i(\bar{t}),\ i = 1, \dots, n.
\end{aligned}$$

Let $w = (v_1, \dots, v_n, u_1, \dots, u_n)^T$, then one can rewrite this system as

$$\frac{dw(t)}{dt} = (F_\varepsilon - V_\varepsilon)w(t),$$

where F_ε and V_ε are the matrices defined in (7) and (8), respectively, evaluated in $x_0(\varepsilon)$ whose components are $S_{0,i} + \varepsilon$ for $i = 1, \dots, n$ and 0 in the remaining $2n$ components.

Notice that we can choose $\varepsilon > 0$ sufficient small such that $\rho(F_\varepsilon V_\varepsilon^{-1}) < 1$, and then, from Lemma 3, all the eigenvalues of matrix $(F_\varepsilon - V_\varepsilon)$ have negative real parts. It follows that $\lim_{t\to\infty} w_i(t) = 0$ from any initial conditions in Γ, from which

$$\lim_{t\to\infty} A_i(t) = 0 \quad \text{and} \quad \lim_{t\to\infty} I_i(t) = 0.$$

Thus, for any $\varepsilon > 0$, there exists $\bar{t}_1 > 0$ such that, for all $t \ge \bar{t}_1$, we have

$$A_i(t) < \varepsilon \text{ and } I_i(t) < \varepsilon, \qquad i = 1, \dots, n.$$

From that and the first n equations of system (3), we get that for all $i = 1, \dots, n$ and for $t \geq \bar{t}_1$

$$\frac{dS_i(t)}{dt} \geq \mu_i - \varepsilon \sum_{j=1}^{n} \left(\beta_{ij}^A + \beta_{ij}^I\right) S_i(t) - (\mu_i + \nu_i + \gamma) S_i(t) + \gamma(1 - 2\varepsilon).$$

The comparison system

$$\frac{dz_i(t)}{dt} = \mu_i - \varepsilon \sum_{j=1}^{n} \left(\beta_{ij}^A + \beta_{ij}^I\right) z_i(t) - (\mu_i + \nu_i + \gamma) z_i(t) + \gamma(1 - 2\varepsilon), \qquad i = 1, \dots, n,$$

has a GAS equilibrium

$$z_0 = \left(\frac{\mu_1 + \gamma(1 - 2\varepsilon)}{\varepsilon\left(\sum_{j=1}^{n} \beta_{1j}^A + \beta_{1j}^I\right) + (\mu_1 + \nu_1 + \gamma)}, \dots, \frac{\mu_n + \gamma(1 - 2\varepsilon)}{\varepsilon\left(\sum_{j=1}^{n} \beta_{nj}^A + \beta_{nj}^I\right) + (\mu_n + \nu_n + \gamma)} \right).$$

Thus, we get that for any $\zeta > 0$, there exists $\bar{t}_2 > 0$ such that for all $t \geq \bar{t}_2$,

$$S_i(t) \geq \frac{\mu_i + \gamma(1 - 2\varepsilon)}{\varepsilon\left(\sum_{j=1}^{n} \beta_{ij}^A + \beta_{ij}^I\right) + (\mu_i + \nu_i + \gamma)} - \zeta, \qquad i = 1, \dots, n.$$

This implies that for all $\varepsilon > 0$

$$\liminf_{t \to \infty} S_i(t) \geq \frac{\mu_i + \gamma(1 - 2\varepsilon)}{\varepsilon\left(\sum_{j=1}^{n} \beta_{ij}^A + \beta_{ij}^I\right) + (\mu_i + \nu_i + \gamma)}, \ i = 1, \dots, n.$$

Letting ε go to 0, we have $\liminf_{t \to \infty} S_i(t) \geq S_{0,i}$ for all $i = 1, \dots, n$, which combined with (12) gives us

$$\lim_{t \to \infty} S_i(t) = S_{0,i}, \qquad i = 1, \dots, n.$$

□

3.1 | SAIRS without vaccination

Let us consider the SAIRS model without vaccination, that is, (3) with $\nu_i = 0$, $i = 1, \dots, n$. From (6), the expression of the basic reproduction number is

$$\mathcal{R}_0 = \rho\left(\left(\left(\beta_{ij}^A + \frac{\alpha\beta_{ij}^I}{\delta_I + \mu_i}\right)\frac{1}{\alpha + \delta_A + \mu_i}\right)_{i,j=1,\dots,n}\right), \tag{13}$$

and the components of the DFE (5) become $S_{0,i} = 1, A_{0,i} = I_{0,i} = 0$, for all $i = 1, \dots, n$.

In Theorems 4 and 5, we proved that the DFE is GAS if $R_0 < 1$ and unstable if $R_0 > 1$. In the following theorem, which describe the case when we do not have any vaccination, we are able to prove that the DFE is GAS also when $R_0 = 1$.

Theorem 6. *The DFE x_0 is GAS in Γ for (3) if $\mathcal{R}_0 \leq 1$.*

Proof. To prove the statement, we use the method presented in Shuai and van den Driessche [33].

Rearranging the order of the equations such that the disease compartments can be written as $x = (A_1, \dots, A_n, I_1, \dots, I_n)$, system (3), restricted to these compartments, can be rewritten as

$$x' = (F - V)x - f(x, S),$$

where

$$f(x,S)=\left(\sum_{j=1}^{n}\left(\beta_{1j}^{A}A_j+\beta_{1j}^{I}I_j\right)(S_{0,1}-S_1),\ \dots\ ,\sum_{j=1}^{n}\left(\beta_{nj}^{A}A_j+\beta_{nj}^{I}I_j\right)(S_{0,n}-S_n),0,\ \dots\ ,0\right)\geq 0,$$

and $f(x,S)$ is a vector with non-negative elements for all $(x,S)\in\Gamma$ and $f(x,S_0)=0$, for all $(x,S_0)\in\Gamma$.

Let ω^T be the left eigenvector of M corresponding to the eigenvalue $\mathcal{R}_0$. Note that in our case, the irreducibility assumption for M in Shuai and van den Driessche [33, Theorem 2.2] fails. However, we can show that $\omega>0$. Indeed, let $\omega^T=(\omega_1,\omega_2)$, where ω_1 and ω_2 are both vectors with n components. It is easy to see that ω_1 is the left eigenvector of the non-negative matrix M_1 (10) corresponding to its spectral radius $\rho(M_1)=\mathcal{R}_0$. Since M_1 is irreducible and non-negative, it follows by the Perron–Frobenius theorem that $\omega_1>0$. Moreover, from (9), let

$$M_2=\left(\frac{\beta_{ij}^{I}S_{0,i}}{\delta_I+\mu_i}\right)_{i,j=1,\dots,n},$$

then, we have $\omega_1M_2=\mathcal{R}_0\omega_2$; since $\omega_1M_2>0$ it follows that $\omega_2>0$. Hence, $\omega>0$. Now, consider the following Lyapunov function:

$$Q=\omega^TV^{-1}x.$$

By differentiating Q along the solution of (3), we obtain

$$\begin{aligned}Q'&=\omega^TV^{-1}x'\\&=\omega^TV^{-1}(F-V)x-\omega^TV^{-1}f(x,S)\\&=(\mathcal{R}_0-1)\omega^Tx-\omega^TV^{-1}f(x,S).\end{aligned}$$

Since $\omega^T>0$, $V^{-1}\geq 0$ and $f(x,S)\geq 0$, it follows that $Q'\leq(\mathcal{R}_0-1)\omega^Tx$, Hence, $Q'\leq 0$ provided $\mathcal{R}_0\leq 1$. Moreover, $Q'=0$ if $x=0$ or $S_i=S_{0,i}$, for all $i=1,\dots,n$, but this last case still implies $x=0$. It can be verified that the only invariant set where $x=0$ is the singleton $\{x_0\}$. Hence, by LaSalle's invariance principle, the DFE x_0 is GAS if $\mathcal{R}_0\leq 1$. □

4 | EXISTENCE AND UNIQUENESS OF EE

To prove the existence and uniqueness of an EE point, we recall the following definition and theorem from Hethcote and Thieme [34].

Definition 7. A function $F(x):\mathbb{R}_+^n\to\mathbb{R}_+^n$ is called strictly sublinear if for fixed $x\in(0,\infty)^n$ and fixed $r\in(0,1)^n$, there exists an $\varepsilon>0$ such that $F(rx)\geq(1+\varepsilon)rF(x)$, where $\geq$ denotes the pointwise ordering in $\mathbb{R}^n$.

Theorem 8 (Theorem 2.2 [34]). *Let $F(x):\mathbb{R}_+^n\to\mathbb{R}_+^n$ be a continuous, monotone nondecreasing, strictly sublinear, and bounded function. Let $F(0)=0$ and $J_F(0)$ exist and be irreducible, where J_F is the Jacobian matrix of F. Then, $F(x)$ does not have a nontrivial fixed point on the boundary of $\mathbb{R}_+^n$. Moreover, $F(x)$ has a positive fixed point if and only if $\rho(J_F(0))>1$. If there is a positive fixed point, then it is unique.*

By using the above result, we can prove the following theorem.

Theorem 9. *System (3) admits a unique EE $x^*:=\left(S_1^*,A_1^*,I_1^*,\ \dots\ ,S_n^*,A_n^*,I_n^*\right)$ in $\ddot{\Gamma}$ if and only if $\mathcal{R}_0>1$.*

Proof. An equilibrium point is a solution of the nonlinear equations obtained by setting the right-hand side of Equation (3) equal to zero. Then, the following must hold:

$$\mu_i-\sum_{j=1}^{n}\left(\beta_{ij}^{A}A_j^*+\beta_{ij}^{I}I_j^*\right)S_i^*-(\mu_i+\nu_i+\gamma)S_i^*+\gamma(1-A_i^*-I_i^*)=0,\tag{14}$$

$$\sum_{j=1}^{n}\left(\beta_{ij}^{A}A_j^* + \beta_{ij}^{I}I_j^*\right)S_i^* - (\alpha+\delta_A+\mu_i)A_i^* = 0, \tag{15}$$

$$\alpha A_i^* - (\delta_I+\mu_i)I_i^* = 0, \tag{16}$$

for $i = 1, 2, \dots, n$. By excluding as solution the DFE (5), we assume $A_i^* > 0$, for some $1 \le i \le n$. From (16), we immediately obtain

$$I_i^* = \frac{\alpha}{\delta_I+\mu_i}A_i^* =: K_iA_i^*, \tag{17}$$

for all $i = 1, 2, \dots, n$. Substituting (17) in (15), we obtain

$$S_i^* = \frac{(\alpha+\delta_A+\mu_i)A_i^*}{\sum_{j=1}^{n}\left(\beta_{ij}^{A}+\beta_{ij}^{I}K_j\right)A_j^*}. \tag{18}$$

By our assumption on x^*, the denominator of (18) is strictly positive. Lastly, substituting (17) and (18) into (14), we obtain

$$\mu_i - (\alpha+\delta_A+\mu_i)A_i^* - (\mu_i+\nu_i+\gamma)\frac{(\alpha+\delta_A+\mu_i)A_i^*}{\sum_{j=1}^{n}\left(\beta_{ij}^{A}+\beta_{ij}^{I}K_j\right)A_j^*} + \gamma\left(1-(1+K_i)A_i^*\right) = 0,$$

which can be rearranged to give

$$A_i^* = \frac{(\mu_i+\gamma)\sum_{j=1}^{n}(\beta_{ij}^{A}+\beta_{ij}^{I}K_j)A_j^*}{(\mu_i+\nu_i+\gamma)(\alpha+\delta_A+\mu_i) + (\alpha+\delta_A+\mu_i+\gamma+\gamma K_i)\sum_{j=1}^{n}\left(\beta_{ij}^{A}+\beta_{ij}^{I}K_j\right)A_j^*}.$$

We can collect $(\mu_i+\nu_i+\gamma)(\alpha+\delta_A+\mu_i)$ and $(\mu_i+\gamma)$ in both the numerator and denominator, to obtain

$$A_i^* = \frac{\sum_{j=1}^{n}(M_1)_{i,j}A_j^*}{1+(\mu_i+\gamma)^{-1}(\alpha+\delta_A+\mu_i+\gamma+\gamma K_i)\sum_{j=1}^{n}(M_1)_{i,j}A_j^*}, \tag{19}$$

with M_1 as in (6).

Define a function $H = (h_1, \dots, h_n) : \mathbb{R}_+^n \to \mathbb{R}_+^n$, in the following way:

$$h_i(y) = \frac{\sum_{j=1}^{n}(M_1)_{i,j}y_j}{1+(\mu_i+\gamma)^{-1}(\alpha+\delta_A+\mu_i+\gamma+\gamma K_i)\sum_{j=1}^{n}(M_1)_{i,j}y_j}, \qquad i = 1, 2, \dots, n.$$

Then, since

$$\frac{\partial h_j}{\partial y_i} > 0,$$

for all $i, j = 1, 2, \dots, n$, H is monotonically increasing in all its components. Moreover, $J_H(0) = M_1$ that is a non-negative and irreducible matrix and the function $H(x)$ is bounded and strictly sublinear with

$$\varepsilon = \min_i \frac{(1-r)\xi_i\sum_{j=1}^{n}(M_1)_{i,j}y_j}{1+r\xi_i\sum_{j=1}^{n}(M_1)_{i,j}y_j},$$

where

$$\xi_i = (\mu_i+\gamma)^{-1}(\alpha+\delta_A+\mu_i+\gamma+\gamma K_i).$$

Thus, by Theorem 8, we have that system (3) has an unique EE in $\ddot{\Gamma}$. □

Remark 1. From Equation (17), we can note that since $I_i^* < 1$, we have that $A_i^* < \frac{\delta_I+\mu_i}{\alpha}$.

4.1 | Local asymptotic stability

In this section, we investigate the local asymptotic stability of the EE.

Theorem 10. *Assume $\mathcal{R}_0 > 1$ and that for any fixed j, $\beta_{ij}^I = h_j\beta_{ij}^A$ for all $i = 1, \dots, n$. Moreover, let us assume that*

$$\delta_A > \nu_i,\ \delta_I > \nu_i, \quad \text{and} \quad (\delta_I - \nu_i)\alpha \le 2(\mu_i + 2\nu_i + \gamma + \delta_I)\sqrt{((\mu_i + \nu_i + \gamma)(\delta_I + \nu_i))} + (\mu_i + 2\nu_i + \gamma + \delta_I)^2,$$

for $i = 1, \dots, n$. Then, the EE $x^* := \left(S_1^*, A_1^*, I_1^*, \dots, S_n^*, A_n^*, I_n^*\right)$ is local asymptotically stable.

Proof. Usually, the asymptotic local stability of the EE point is studied by linearizing system (4) around that point. However, it is known that the EE is asymptotically stable if the linearized system $\frac{dy}{dt} = J_f(x^*)y$ has no solution of the form $y(t) = Ye^{zt}$ with

$$Y = (U_1, \dots, U_n, V_1, \dots, V_n, W_1, \dots, W_n) \in \mathbb{C}^{3n},$$

$z \in \mathbb{C}$, $\mathrm{Re}z \ge 0$, that is, it means that $zY = J_f(x^*)Y$ with $Y \in \mathbb{C}^n\backslash\{0\}, z \in \mathbb{C}$ implies $\mathrm{Re}z < 0$ [8, 34]. To prove our statement with this strategy, we consider the following system, equivalent to (4):

$$\frac{dx}{dt} = f(x(t)),$$

where $x(t) = (A_1(t), I_1(t), R_1(t), \dots, A_n(t), I_n(t), R_n(t))$ and $f(x(t)) = (f_1(x(t)), f_2(x(t)), \dots, f_{3n}(x(t)))$, with

$$\begin{aligned}
f(x_1(t)) &= \sum_{j=1}^{n}(\beta_{ij}^A A_j(t) + \beta_{ij}^I I_j(t))(1 - A_i(t) - I_i(t) - R_i(t)) - (\alpha + \mu_i + \delta_A)A_i(t),\\
f(x_2(t)) &= \alpha A_i(t) - (\mu_i + \delta_I)I_i(t),\\
f(x_3(t)) &= \delta_A A_i(t) + \delta_I I_i(t) + \nu_i(1 - A_i(t) - I_i(t) - R_i(t)) - (\mu_i + \gamma)R_i(t).
\end{aligned}$$

Now, to prove the asymptotic local stability of x^*, we consider the following equations:

$$\begin{aligned}
zU_i &= \left(1 - A_i^* - I_i^* - R_i^*\right)\sum_{j=1}^{n}\left(\beta_{ij}^A U_j + \beta_{ij}^I V_j\right) - \sum_{j=1}^{n}\left(\beta_{ij}^A A_j^* + \beta_{ij}^I I_j^*\right)(U_i + V_i + W_i) - (\alpha + \mu_i + \delta_A)U_i,\\
zV_i &= \alpha U_i - (\delta_I + \mu_i)V_i,\\
zW_i &= (\delta_A - \nu_i)U_i + (\delta_I - \nu_i)V_i - (\mu_i + \nu_i + \gamma)W_i, \qquad i = 1, \dots, n,
\end{aligned} \tag{20}$$

with $U_i, V_i, W_i, z \in \mathbb{C}$. We proceed by assuming that $\mathrm{Re}z \ge 0$ and showing that this assumption leads to a contradiction.

From the second and third equation of (20), we have, respectively,

$$V_i = \frac{\alpha}{z + \delta_I + \mu_i}U_i := K_i^1(z)U_i, \tag{21}$$

and

$$W_i = \left[\frac{1}{z + \mu_i + \nu_i + \gamma}\left((\delta_A - \nu_i) + \frac{(\delta_I - \nu_i)\alpha}{z + \delta_I + \nu_i}\right)\right]U_i := K_i^2(z)U_i. \tag{22}$$

Now, considering the assumption that fixed j, $\beta_{ij}^I = h_j\beta_{ij}^A$ for all $i = 1, \dots, n$, and replacing (21) and (22) in the first equation of (20), we obtain

$$zU_i = S_i^*\sum_{j=1}^{n}\beta_{ij}^A\left(1 + h_jK_j^1(z)\right)U_j - \left[\sum_{j=1}^{n}\beta_{ij}^A\left(A_j^* + h_jI_j^*\right)\left(1 + K_i^1(z) + K_i^2(z)\right) + (\alpha + \mu_i + \delta_A)\right]U_i,$$

from which

$$\left[1+\frac{1}{\alpha+\mu_i+\delta_A}\left(z+\sum_{j=1}^{n}\beta_{ij}^{A}\left(A_j^*+h_jI_j^*\right)\left(1+K_i^1(z)+K_i^2(z)\right)\right)\right]U_i=\frac{S_i^*}{\alpha+\mu_i+\delta_A}\sum_{j=1}^{n}\beta_{ij}^{A}\left(1+h_jK_j^1(z)\right)U_j. \tag{23}$$

Now, let

$$\eta_i(z)=\frac{1}{\alpha+\mu_i+\delta_A}\left(z+\sum_{j=1}^{n}\beta_{ij}^{A}\left(A_j^*+h_jI_j^*\right)\left(1+K_i^1(z)+K_i^2(z)\right)\right),$$

and consider the following transformation:

$$U_j=\left(1+\frac{h_j\alpha}{z+\delta_I+\mu_j}\right)^{-1}\left(1+\frac{h_j\alpha}{\delta_I+\mu_j}\right)\tilde{U}_j.$$

Then, we get

$$(1+\eta_i(z))\left(1+\frac{h_i\alpha}{z+\delta_I+\mu_i}\right)^{-1}\left(1+\frac{h_i\alpha}{\delta_I+\mu_i}\right)\tilde{U}_i=\frac{S_i^*}{\alpha+\mu_i+\delta_A}\sum_{j=1}^{n}\beta_{ij}^{A}\left(1+\frac{h_j\alpha}{\delta_I+\mu_j}\right)\tilde{U}_j. \tag{24}$$

Now, let us note that if $\mathrm{Re}z\geq 0$, then

$$\mathrm{Re}\left(\left(1+\frac{h_i\alpha}{z+\delta_I+\mu_i}\right)^{-1}\left(1+\frac{h_i\alpha}{\delta_I+\mu_i}\right)\right)\geq 1. \tag{25}$$

Hence, we can rewrite (24) in the following form:

$$(1+\eta_i(z))\,(1+\tilde{\eta}_i(z))\tilde{U}_i=(C\tilde{U})_i, \tag{26}$$

where $C=(c_{ij})$ with

$$c_{ij}=\frac{S_i^*}{\alpha+\mu_i+\delta_A}\sum_{j=1}^{n}\beta_{ij}^{A}\left(1+\frac{h_j\alpha}{\delta_I+\mu_j}\right),\qquad i,j=1,\ \dots\ ,n.$$

From (25), we have that $\mathrm{Re}\tilde{\eta}_i(z)\geq 0$. Moreover, the following claim, whose proof is given in Appendix A1, holds:

Claim 11. If $\mathrm{Re}z\geq 0$, then $\mathrm{Re}\eta_i(z)>0$.

Now, let us note that C is a non-negative matrix and that $A^*=CA^*$, where $A^*=(A_1^*,\ \dots\ ,A_n^*)$. Let

$$\eta(z)=\inf\{\mathrm{Re}\eta_i(z),i=1,\ \dots\ ,n\},\qquad\text{and}\qquad|\tilde{U}|=(|\tilde{U}_1|,\ \dots\ ,|\tilde{U}_n|),$$

and taking the absolute values in (26), we get

$$(1+\eta(z))|\tilde{U}|\leq C|\tilde{U}|. \tag{27}$$

It is easy to verify that if $\mathrm{Re}z\geq 0$, then $\mathrm{Re}\eta_i(z)>0$ for all i, hence $\eta(z)>0$. Now, we define ϵ to be the minimum value for which $|\tilde{U}|\leq\epsilon A^*$. Since the components of A^* belong to $(0,1)$, $\epsilon<\infty$. Hence, by (27), $(1+\eta(z))|\tilde{U}|\leq C|\tilde{U}|\leq\epsilon CA^*=\epsilon A^*$. This inequality contradicts the minimality of ϵ because $\eta(z)>0$ if $\mathrm{Re}z\geq 0$; thus, we can conclude that $\mathrm{Re}z<0$ and the equilibrium is stable. □

As in Ottaviano et al. [16], we conjecture that some, if not all, these technical assumptions could be relaxed, as our numerical simulations suggest. However, the techniques we use in this paper require such assumptions on the parameters in order to reach a result, and multi-group models often require cumbersome hypotheses [35–37].

5 | GLOBAL STABILITY OF THE EE

In this section, we first discuss the persistence of the disease, then we investigate the global stability property of the EE for some variations of the original model (1).

Definition 12. System (3) is said to be uniformly persistent if there exists a constant $0 < \varepsilon < 1$ such that any solution $x(t)$ with $x(0) \in \ddot{\Gamma}$ satisfies

$$\min\left\{\liminf_{t\to\infty} S_i(t),\ \liminf_{t\to\infty} A_i(t),\ \liminf_{t\to\infty} I_i(t)\right\} \geq \varepsilon,\ i = 1, \dots, n. \tag{28}$$

Theorem 13. *If $\mathcal{R}_0 > 1$, system (3) is uniformly persistent.*

Proof. From Theorem 9, we know that DFE x_0 is the unique equilibrium of (3) on $\partial\Gamma$, that is, the largest invariant set on $\partial\Gamma$ is the singleton $\{x_0\}$, which is isolated. If $\mathcal{R}_0 > 1$, we know from Theorem 4 that x_0 is unstable. Then, by using Freedman et al. [38, Theorem 4.3], and similar arguments in Li et al. [39, Proposition 3.3], we can assert that the instability of x_0 implies the uniform persistence of (3). □

5.1 | Global stability of the EE in the SAIR model

In this section, we study the global asymptotic stability of the EE of the SAIR model, which describes the dynamic of a disease which confers permanent immunity (i.e., $\gamma = 0$). The dynamic of an SAIR model of this type is described by the following system of equations:

$$\begin{aligned}
\frac{dS_i(t)}{dt} &= \mu_i - \sum_{j=1}^{n}\left(\beta_{ij}^A A_j(t) + \beta_{ij}^I I_j(t)\right) S_i(t) - (\mu_i + \nu_i) S_i(t),\\
\frac{dA_i(t)}{dt} &= \sum_{j=1}^{n}\left(\beta_{ij}^A A_j(t) + \beta_{ij}^I I_j(t)\right) S_i(t) - (\alpha + \delta_A + \mu_i) A_i(t),\\
\frac{dI_i(t)}{dt} &= \alpha A_i(t) - (\delta_I + \mu_i) I_i(t), \qquad i = 1, \dots, n.
\end{aligned} \tag{29}$$

The basic reproduction number is derived by substituting γ with 0 in (6):

$$\mathcal{R}_0 = \rho\left(\left(\left(\beta_{ij}^A + \frac{\alpha\beta_{ij}^I}{(\delta_I + \mu_i)}\right)\frac{\mu_i}{(\mu_i + \nu_i)(\alpha + \delta_A + \mu_i)}\right)_{i,j=1,\dots,n}\right).$$

If $\mathcal{R}_0 > 1$, system (29) has a unique equilibrium in $\ddot{\Gamma}$, which satisfies

$$\mu_i = \sum_{j=1}^{n}\left(\beta_{ij}^A A_j^* + \beta_{ij}^I I_j^*\right) S_i^* + (\mu_i + \nu_i) S_i^*, \tag{30}$$

$$(\alpha + \delta_A + \mu_i) A_i^* = \sum_{j=1}^{n}\left(\beta_{ij}^A A_j^* + \beta_{ij}^I I_j^*\right) S_i^*, \tag{31}$$

$$\alpha A_i^* = (\delta_I + \mu_i) I_i^*. \tag{32}$$

Theorem 14. *The EE x^* is GAS in $\ddot{\Gamma}$ if $\mathcal{R}_0 > 1$.*

Proof. In order to prove the statement, we use a graph-theoretic approach as in Shuai and van den Driessche [33] to establish the existence of a Lyapunov function. Let us define

$$\tilde{s}_i = \frac{S_i}{S_i^*}, \qquad \tilde{a}_i = \frac{A_i}{A_i^*}, \qquad \tilde{\zeta}_i = \frac{I_i}{I_i^*},$$

and $g(x) := x-1-\ln(x) \geq 0$ for all $x > 0$. Let $V_i = V_{i,1}+V_{i,2}$, where $V_{i,1} = S_i^* \cdot g(\tilde{s}_i)$, $V_{i,2} = A_i^* \cdot g(\tilde{a}_i)$, and $V_{n+i} = I_i^* \cdot g(\tilde{\zeta}_i)$, for $i = 1, \dots, n$.

Define $h(x) := -g(x) - 1 = -x + \ln(x)$ and note that

$$\left(1 - \frac{1}{x}\right)(x-1) = -2 + x + \frac{1}{x} = -1 + x - \ln x - 1 + \frac{1}{x} - \ln\frac{1}{x} = g(x) + g\left(\frac{1}{x}\right). \tag{33}$$

Substituting (30), (31), and (32) in (29), we obtain

$$\begin{aligned}
\frac{dS_i(t)}{dt} &= -S_i^*(\mu_i + \nu_i)(\tilde{s}_i - 1) + \sum_{j=1}^{n}\left(\beta_{ij}^A\left(A_j^*S_i^* - A_jS_i\right) + \beta_{ij}^I\left(I_j^*S_i^* - I_jS_i\right)\right),\\
\frac{dA_i(t)}{dt} &= \sum_{j=1}^{n}\left(\left(\beta_{ij}^A A_j + \beta_{ij}^I I_j\right)S_i - \left(\beta_{ij}^A A_j^* + \beta_{ij}^I I_j^*\right)S_i^*\frac{A_i}{A_i^*}\right),\\
\frac{dI_i(t)}{dt} &= \alpha\left(A_i - A_i^*\frac{I_i}{I_i^*}\right), \qquad i = 1, \dots, n.
\end{aligned}$$

For $i = 1, \dots, n$, differentiating V_i along the solutions of (29) and using (33), we have

$$\begin{aligned}
\frac{dV_{i,1}}{dt} &= \left(1 - \frac{1}{\tilde{s}_i}\right)\frac{dS_i(t)}{dt}\\
&= \left(1 - \frac{1}{\tilde{s}_i}\right)\left[-S_i^*(\mu_i + \nu_i)(\tilde{s}_i - 1) + \sum_{j=1}^{n}\left(\beta_{ij}^A\left(A_j^*S_i^* - A_jS_i\right) + \beta_{ij}^I\left(I_j^*S_i^* - I_jS_i\right)\right)\right]\\
&= \left(1 - \frac{1}{\tilde{s}_i}\right)\left[-S_i^*(\mu_i + \nu_i)(\tilde{s}_i - 1) + \sum_{j=1}^{n}\left(\beta_{ij}^A A_j^*S_i^*\left(1 - \tilde{a}_j\tilde{s}_i\right) + \beta_{ij}^I I_j^*S_i^*\left(1 - \tilde{\zeta}_j\tilde{s}_i\right)\right)\right]\\
&= -S_i^*(\mu_i + \nu_i)\frac{(\tilde{s}_i - 1)^2}{S_i} + \sum_{j=1}^{n}\left(\beta_{ij}^A A_j^*S_i^*\left(1 - \tilde{a}_j\tilde{s}_i - \frac{1}{\tilde{s}_i} + \tilde{a}_j\right) + \beta_{ij}^I I_j^*S_i^*\left(1 - \tilde{\zeta}_j\tilde{s}_i - \frac{1}{\tilde{s}_i} + \tilde{\zeta}_j\right)\right),
\end{aligned} \tag{34}$$

$$\begin{aligned}
\frac{dV_{i,2}}{dt} &= \left(1 - \frac{1}{\tilde{a}_i}\right)\frac{dA_i(t)}{dt}\\
&= \left(1 - \frac{1}{\tilde{a}_i}\right)\left[\sum_{j=1}^{n}\left(\left(\beta_{ij}^A A_j + \beta_{ij}^I I_j\right)S_i - \left(\beta_{ij}^A A_j^* + \beta_{ij}^I I_j^*\right)S_i^*\frac{A_i}{A_i^*}\right)\right]\\
&= \left(1 - \frac{1}{\tilde{a}_i}\right)\left[\sum_{j=1}^{n}\left(\beta_{ij}^A A_j^*S_i^*\left(\tilde{a}_j\tilde{s}_i - \tilde{a}_i\right) + \beta_{ij}^I I_j^*S_i^*\left(\tilde{\zeta}_j\tilde{s}_i - \tilde{a}_i\right)\right)\right]\\
&= \sum_{j=1}^{n}\left(\beta_{ij}^A A_j^*S_i^*\left(\tilde{a}_j\tilde{s}_i - \tilde{a}_i - \frac{\tilde{a}_j\tilde{s}_i}{\tilde{a}_i} + 1\right) + \beta_{ij}^I I_j^*S_i^*\left(\tilde{\zeta}_j\tilde{s}_i - \tilde{a}_i - \frac{\tilde{\zeta}_j\tilde{s}_i}{\tilde{a}_i} + 1\right)\right).
\end{aligned} \tag{35}$$

Thus, from (34) and (35), we obtain

$$\frac{dV_i}{dt} \leq \sum_{j=1}^{n}\left(\beta_{ij}^A A_j^*S_i^*\left(2 - \frac{1}{\tilde{s}_i} + \tilde{a}_j - \tilde{a}_i - \frac{\tilde{a}_j\tilde{s}_i}{\tilde{a}_i}\right) + \beta_{ij}^I I_j^*S_i^*\left(2 - \frac{1}{\tilde{s}_i} + \tilde{\zeta}_j - \tilde{a}_i - \frac{\tilde{\zeta}_j\tilde{s}_i}{\tilde{a}_i}\right)\right). \tag{36}$$

Using the fact that $1 - x \leq -\ln(x)$, we can write

$$2 - \frac{1}{\tilde{s}_i} + \tilde{a}_j - \tilde{a}_i - \frac{\tilde{a}_j \tilde{s}_i}{\tilde{a}_i} \leq \tilde{a}_j - \tilde{a}_i - \ln\left(\frac{1}{\tilde{s}_i}\right) - \ln\left(\frac{\tilde{a}_j \tilde{s}_i}{\tilde{a}_i}\right) = h(\tilde{a}_i) - h(\tilde{a}_j),$$
$$2 - \frac{1}{\tilde{s}_i} + \tilde{\zeta}_j - \tilde{a}_i - \frac{\tilde{\zeta}_j \tilde{s}_i}{\tilde{a}_i} \leq \tilde{\zeta}_j - \tilde{a}_i - \ln\left(\frac{1}{\tilde{s}_i}\right) - \ln\left(\frac{\tilde{\zeta}_j \tilde{s}_i}{\tilde{a}_i}\right) = h(\tilde{a}_i) - h(\tilde{\zeta}_j).$$

Thus, we obtain

$$\frac{dV_i}{dt} \leq \sum_{j=1}^{n} \left(\beta_{ij}^A A_j^* S_i^* (h(\tilde{a}_i) - h(\tilde{a}_j)) + \beta_{ij}^I I_j^* S_i^* (h(\tilde{a}_i) - h(\tilde{i}_j))\right) =: \sum_{j=1}^{2n} \tilde{\beta}_{ij} G_{i,j},$$

where

$$\tilde{\beta}_{ij} = \begin{cases} \beta_{ij}^A A_j^* S_i^*, & 1 \leq j \leq n, \\ \beta_{i\ j-n}^I I_{j-n}^* S_i^*, & n+1 \leq j \leq 2n, \end{cases} \text{ and } G_{ij} = \begin{cases} h(\tilde{a}_i) - h(\tilde{a}_j), & 1 \leq j \leq n, \\ h(\tilde{a}_i) - h(\tilde{\zeta}_{j-n}), & n+1 \leq j \leq 2n. \end{cases}$$

Moreover, for all $i = 1, \ldots, n$,

$$\begin{aligned} \frac{dV_{n+i}}{dt} &= \left(1 - \frac{1}{\tilde{\zeta}_i}\right) \frac{dI_i}{dt} = \alpha \left(1 - \frac{1}{\tilde{\zeta}_i}\right) \left[A_i - A_i^* \frac{I_i}{I_i^*}\right] \\ &= \alpha A_i^* \left(1 - \frac{1}{\tilde{\zeta}_i}\right) (\tilde{a}_i - \tilde{\zeta}_i) = \alpha A_i^* \left(\tilde{a}_i - \tilde{\zeta}_i - \frac{\tilde{a}_i}{\tilde{\zeta}_i} + 1\right), \end{aligned} \tag{37}$$

and again, using the fact that $1 - x \leq -\ln(x)$, we have

$$1 + \tilde{a}_i - \tilde{\zeta}_i - \frac{\tilde{a}_i}{\tilde{\zeta}_i} \leq \tilde{a}_i - \tilde{\zeta}_i - \ln\left(\frac{\tilde{a}_i}{\tilde{\zeta}_i}\right) = h(\tilde{\zeta}_i) - h(\tilde{a}_i).$$

Thus,

$$\frac{dV_{n+i}}{dt} \leq \alpha A_i^* (h(\tilde{\zeta}_i) - h(\tilde{a}_i)) =: \tilde{\beta}_{n+i\ i} G_{n+i\ i}. \tag{38}$$

We can construct a weighted digraph $\mathcal{G}$, associated with the weight matrix $\tilde{B} = (\tilde{\beta}_{ij})_{i,j=1,\ldots,2n}$, with $\tilde{\beta}_{ij} > 0$ as defined above and zero otherwise; see Figure 2. Let us note that, from Assumption 1, the digraph $(\mathcal{G}, \tilde{B})$ is strongly connected. Since $G_{i\ n+j} + G_{n+j\ j} = -\tilde{a}_i + \ln(\tilde{a}_i) + \tilde{a}_j - \ln(\tilde{a}_j) = G_{ij}$, $i, j = 1, \ldots, n$, it can be verified that each directed cycle C of $(\mathcal{G}, \tilde{B})$ has $\sum_{(s,r)\in\mathcal{E}(C)} G_{rs} = 0$, where $\mathcal{E}(C)$ denotes the arc set of the directed cycle C. Thus, the assumptions of Shuai and van den Driessche [33, Theorem 3.5] hold; hence, the function

$$V = \sum_{i=1}^{n} \left(c_i V_i + c_{n+i} V_{n+i}\right),$$

for constants $c_i > 0$ defined as in Shuai and van den Driessche [33, Proposition 3.1], satisfies $\frac{dV}{dt} \leq 0$, meaning that V is a Lyapunov function for system (29). It can be verified that the largest compact invariant set in which $\frac{dV}{dt} = 0$ is the singleton $\{x^*\}$. Hence, our claim follows by LaSalle's invariance principle [40]. □

Remark 2. We observe that the proof of Theorem 14 also holds for the case $\delta_A = 0$ in system (3). That is to say, for a model with two stages of infection I_1 and I_2, in which from the first class of infection one passes to the second at the rate α and one cannot directly pass into the compartment of recovered individuals. Then, from the second stage of infection, one can recover at the rate δ_{I_2}. It is known that, if $\alpha = \delta_{I_2}$, the length of the infectious period follows a gamma distribution; otherwise, the resulting distribution is not a standard one. Moreover, we remark that Theorem 14 only requires $\mathcal{R}_0 > 1$, and no additional conditions on the parameters, despite the complexity of the model under study. Models with multiple infected compartments have been studied, for example, in previous studies [41–43].

5.2 | Global stability of the SAIRS model when $\delta_A = \delta_I =: \delta$

In the $\delta_A = \delta_I =: \delta$ case, from (6), we have

$$\mathcal{R}_0 = \rho\left(\left(\left(\beta_{ij}^A + \frac{\alpha\beta_{ij}^I}{(\delta+\mu_i)}\right)\frac{\gamma+\mu_i}{(\gamma+\mu_i+\nu_i)(\alpha+\delta+\mu_i)}\right)_{i,j=1,\dots,n}\right).$$

If $\mathcal{R}_0 > 1$, system (1) with $\delta_A = \delta_I =: \delta$ has a unique equilibrium in $\ddot{\Gamma}$, which satisfies

$$\begin{aligned}
\mu_i &= \sum_{j=1}^{n}\left(\beta_{ij}^A A_j^* + \beta_{ij}^I I_j^*\right)S_i^* + (\mu_i+\nu_i)S_i^* - \gamma R_i^*,\\
(\alpha+\delta+\mu_i)A_i^* &= \sum_{j=1}^{n}\left(\beta_{ij}^A A_j^* + \beta_{ij}^I I_j^*\right)S_i^*,\\
\alpha A_i^* &= (\delta+\mu_i)I_i^*,\\
\nu_i S_i^* &= -\delta(A_i^* + I_i^*) + (\gamma+\mu_i)R_i^*.
\end{aligned} \tag{39}$$

Theorem 15. *Assume that $(\mu_i+\nu_i)S_i^* \geq \gamma R_i^*$ and $\delta > \nu_i$, for each $i = 1, \dots, n$. Then, the EE x^* is GAS in $\ddot{\Gamma}$ if $\mathcal{R}_0 > 1$.*

Proof. Let $\tilde{s}_i, \tilde{a}_i, \tilde{\zeta}_i, V_i$, and V_{n+i} as in Theorem 14. Let us define $\tilde{r}_i = \frac{R_i}{R_i^*}$ and

$$W_i = \frac{\gamma}{S_i^*(\delta-\nu_i)}\frac{\left(R_i - R_i^*\right)^2}{2}, \qquad i = 1, \dots, n.$$

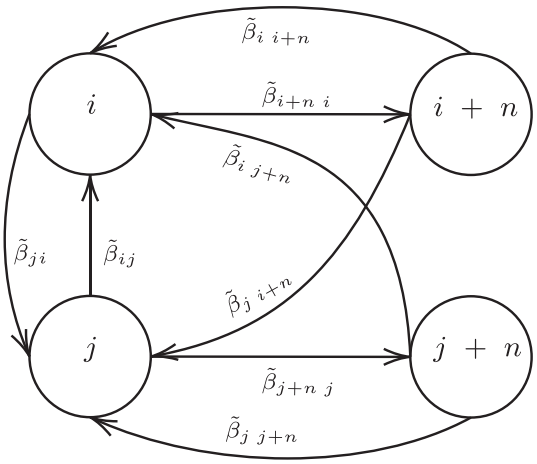

FIGURE 2 The weighted digraph $(G, \tilde{B})$ constructed for system (29)

TABLE 1 Values of the parameters used in the simulations: $\beta_{ii}^A = 0.8$, which we reduced to $\beta_{ij}^A = 0.4$ if $i \neq j$, to model a lower inter-community spreading; $\beta_{ii}^I = 0.95$ and $\beta_{ij}^I = 0.475$ if $i \neq j$; $\mu_i = 1/(70 \cdot 365)$, meaning an average lifespan of 70 years for all i; $\nu_i = 0.01$, meaning 1% of the susceptible population is vaccinated every day for all i; $\gamma = 0.02$, meaning an average immunity of 50 days; $\delta_A = 0.1$, $\delta_I = 0.51$, $\alpha = 0.8$.

β_{ii}^A	β_{ij}^A	β_{ii}^I	β_{ij}^I	μ_i	ν_i	γ	δ_A	δ_I	α
0.8	0.4	0.95	0.475	$1/(70 \cdot 365)$	0.01	0.02	0.1	0.51	0.8

By using Equation (39), and differentiating along the solution of (1) with $\delta_A = \delta_I =: \delta$, we obtain

$$\begin{aligned}\frac{dV_{i,1}}{dt} &= \left(1-\frac{1}{\tilde{s}_i}\right)\frac{dS_i(t)}{dt} = \left(1-\frac{1}{\tilde{s}_i}\right)\left[-S_i^*(\mu_i+\nu_i)(\tilde{s}_i-1)+\gamma R_i^*(\tilde{r}_i-1)+\sum_{j=1}^{n}\left(\beta_{ij}^A A_j^* S_i^*\left(1-\tilde{a}_j\tilde{s}_i\right)+\beta_{ij}^I I_j^* S_i^*\left(1-\tilde{\zeta}_j\tilde{s}_i\right)\right)\right]\\ &= -S_i^*(\mu_i+\nu_i)\left(1-\frac{1}{\tilde{s}_i}\right)(\tilde{s}_i-1)+\gamma R_i^*\left(1-\frac{1}{\tilde{s}_i}\right)(\tilde{r}_i-1)\\ &\quad+\sum_{j=1}^{n}\left(\beta_{ij}^A A_j^* S_i^*\left(1-\tilde{a}_j\tilde{s}_i-\frac{1}{\tilde{s}_i}+\tilde{a}_j\right)+\beta_{ij}^I I_j^* S_i^*\left(1-\tilde{\zeta}_j\tilde{s}_i-\frac{1}{\tilde{s}_i}+\tilde{\zeta}_j\right)\right),\end{aligned} \tag{40}$$

and the derivatives $\frac{dV_{i,2}}{dt}$ and $\frac{dV_{n+i}}{dt}$ as in (35) and (37), respectively. Moreover,

$$\begin{aligned}\frac{dW_i}{dt} &= \frac{\gamma}{S_i^*(\delta-\nu_i)}\left(R_i-R_i^*\right)\frac{dR_i}{dt} = \frac{\gamma}{S_i^*(\delta-\nu_i)}\left(R_i-R_i^*\right)\left[\delta\left(A_i-A_i^*+I_i-I_i^*\right)+\nu_i(S_i-S_i^*)-(\gamma+\mu_i)\left(R_i-R_i^*\right)\right]\\ &= \frac{\gamma}{S_i^*(\delta-\nu_i)}\left(R_i-R_i^*\right)\left[\delta(S_i^*-S_i+R_i^*-R_i)+\nu_i(S_i-S_i^*)-(\gamma+\mu_i)\left(R_i-R_i^*\right)\right]\\ &= \frac{\gamma}{S_i^*(\delta-\nu_i)}R_i^*S_i^*(\nu_i-\delta)(\tilde{s}_i-1)(\tilde{r}_i-1)-(\gamma+\mu_i+\delta)R_i^*(\tilde{r}_i-1)^2,\end{aligned} \tag{41}$$

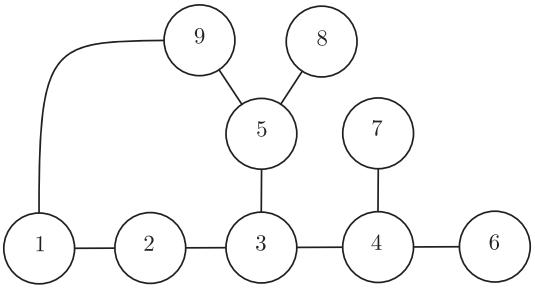

(A) Cycle-tree network, i.e. a tree graph in which we add a cycle linking the first and the last community.

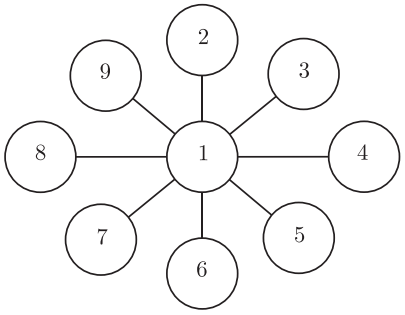

(B) Star network, in which a central community is linked to all the others, and no other connections are present.

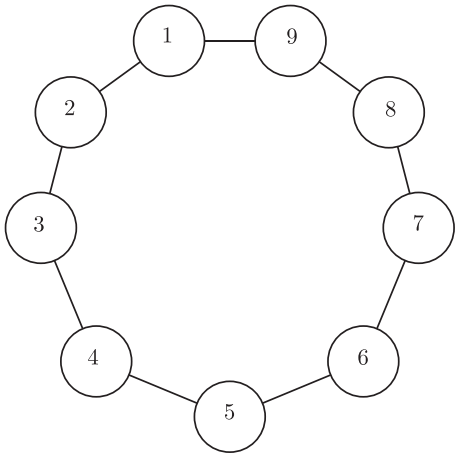

(C) Ring network, in which each community is linked with the previous and next.

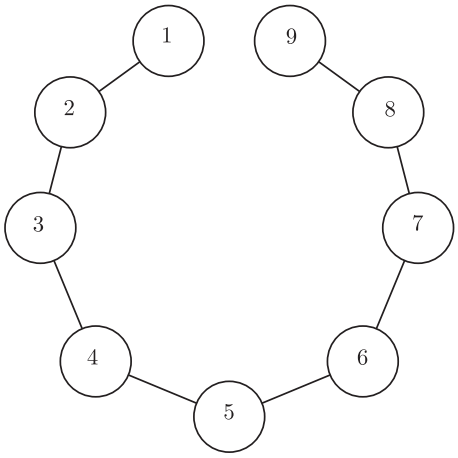

(D) Line network, i.e. the ring network in which we remove the link between the communities 1 and 9.

FIGURE 3 The four different network structures we consider in our numerical simulations. Circles represent the communities, numbered from 1 to 9, corresponding to C1 to C9 in Figures 4–7. Lines represent the links between the various communities. We use lines instead of arrows, since all networks are considered as undirected.

by assumption $\delta > \nu_i$, thus

$$\frac{dW_i}{dt} \leq -\gamma R_i^*(\tilde{s}_i - 1)(\tilde{r}_i - 1). \tag{42}$$

Let us consider the weighted digraph $\mathcal{G}$, the weight matrix $\tilde{B}$, and the functions $G_{i,j}$, for $i, j = 1, \dots, 2n$ defined as in Theorem 14. Consider the following function:

$$V = \sum_{i=1}^{n} (c_i V_i + c_{n+i} V_{n+i}) + \sum_{i=1}^{n} c_i W_i,$$

where the constant $c_i > 0$ are defined as in Shuai and van den Driessche [33, Proposition 3.1]. Then, by following similar steps as in Theorem 14 and from (42), we obtain

$$\begin{aligned}
\frac{dV}{dt} &\leq \sum_{i=1}^{2n}\sum_{j=1}^{2n} c_i \tilde{\beta}_{ij} G_{i,j} - \sum_{i=1}^{n} c_i(\mu_i + \nu_i) S_i^* \left(1 - \frac{1}{\tilde{s}}\right)(\tilde{s}_i - 1) + \sum_{i=1}^{n} c_i \gamma R_i^*(\tilde{r}_i - 1)\left[\left(1 - \frac{1}{\tilde{s}_i}\right) - (\tilde{s}_i - 1)\right] \\
&= \sum_{i=1}^{2n}\sum_{j=1}^{2n} c_i \tilde{\beta}_{ij} G_{i,j} - \sum_{i=1}^{n} c_i(\mu_i + \nu_i) S_i^* \left(1 - \frac{1}{\tilde{s}}\right)(\tilde{s}_i - 1) + \sum_{i=1}^{n} c_i \gamma R_i^*(\tilde{r}_i - 1)\left(1 - \frac{1}{\tilde{s}_i}\right)(1 - \tilde{s}_i) \\
&= \sum_{i=1}^{2n}\sum_{j=1}^{2n} c_i \tilde{\beta}_{ij} G_{i,j} - \sum_{i=1}^{n} c_i \left[(\mu_i + \nu_i) S_i^* + \gamma R_i^*(\tilde{r}_i - 1)\right]\left(1 - \frac{1}{\tilde{s}}\right)(\tilde{s}_i - 1).
\end{aligned} \tag{43}$$

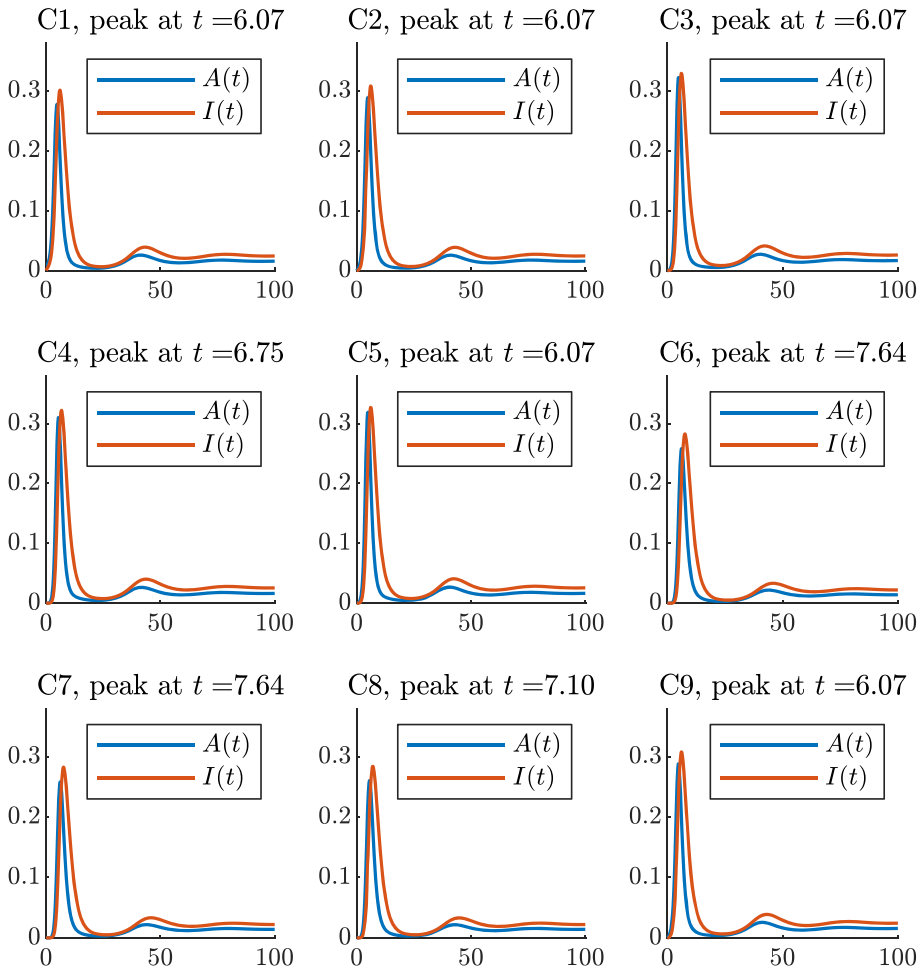

FIGURE 4 Evolution of the epidemic in each community of the cycle-tree network, see Figure 3A. The title of each subplot indicates the community it represents, as well as the peak time of infected individuals. In this setting, from (6), we obtain $\mathcal{R}_0 = 4.37$. Refer to Table 1 for the values of the parameters. [Colour figure can be viewed at wileyonlinelibrary.com]

Now, since it can be verified that over each directed cycle C of $(\mathcal{G}, \tilde{B})$, $\sum_{(s,r)\in\mathcal{E}(C)} G_{rs} = 0$, by following the same arguments in the proof of Shuai and van den Driessche [33, Theorem 3.5], we have that $\sum_{i=1}^{2n}\sum_{j=1}^{2n} c_i \tilde{\beta}_{ij} G_{i,j} = 0$. Moreover, by assumption $(\mu_i + \nu_i)S_i^* \geq \gamma R_i^*$, for each $i = 1, \dots, n$, hence

$$(\mu_i + \nu_i)S_i^* + \gamma R_i^*(r_i - 1) \geq (\mu_i + \nu_i)S_i^* - \gamma R_i^* \geq 0, \qquad i = 1, \dots, n.$$

Thus, we have $\frac{dV}{dt} \leq 0$.

Since the largest compact invariant set in which $\frac{dV}{dt} = 0$ is the singleton $\{x^*\}$, by LaSalle invariance principle, our claim follows. □

Remark 3. Note that if $\nu_i = 0$ for all i, we obtain the same sufficient conditions for the GAS of the EE found for the SIRS model in Muroya et al. [13].

6 | NUMERICAL ANALYSIS

In this section, we explore the role of the network structures in the evolution of the epidemics. The primary criterion for parameter selection is the clarity of the resulting plot. Hence, the simulations were carried out with a set of parameters considered in Ottaviano et al. [16]. These parameters, summarized in Table 1, ensure that $\mathcal{R}_0 > 1$ in all the networks, we consider, whose shapes are represented in Figure 3.

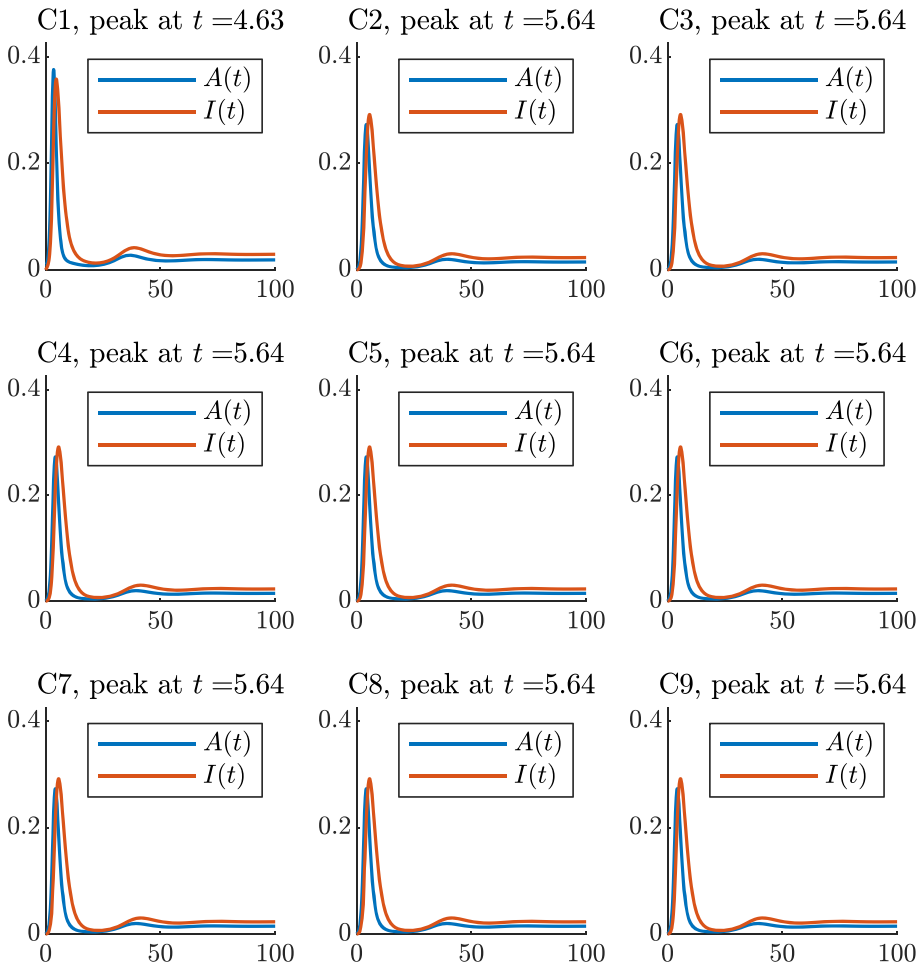

FIGURE 5 Evolution of the epidemic in each community of the star network, see Figure 3B. The title of each subplot indicates the community it represents, as well as the peak time of infected individuals. In this setting, from (6), we obtain $\mathcal{R}_0 = 4.91$. Refer to Table 1 for the values of the parameters. [Colour figure can be viewed at wileyonlinelibrary.com]

In particular, we remark on how sensitive $\mathcal{R}_0$ is on the topology of the network, which is reflected in its adjacency matrix. Indeed, let us consider (6) and let

$$\beta_1 = \min_{i,j} (M_1)_{i,j}, \qquad \text{and} \qquad \beta_2 = \max_{i,j} (M_1)_{i,j}.$$

Let us define $\bar{\mathcal{A}} = \mathcal{A} + I_n$, where $\mathcal{A}$ is the adjacency matrix and n the number of nodes of the network we are considering, respectively. Then, as a consequence of the Perron–Frobenius theorem, the following lower and upper bounds for $\mathcal{R}_0$ hold:

$$\beta_1 \rho(\bar{\mathcal{A}}) \leq \mathcal{R}_0 \leq \beta_2 \rho(\bar{\mathcal{A}}). \tag{44}$$

In the case of the cycle-tree network in Figure 3A, we have $\rho(\mathcal{A}) = 3.2877$, for the star network in Figure 3B, $\rho(\mathcal{A}) = 3.8284$, in the case of the ring network in Figure 3C, $\rho(\mathcal{A}) = 3$, and for the line network in Figure 3D, we have $\rho(\mathcal{A}) = 2.9021$. Consequently, in the star network, we found the largest $\mathcal{R}_0 = 4.91$, for the cycle-tree network, we have $\mathcal{R}_0 = 4.37$. In the other two networks, that is, the ring and the line, we find $\mathcal{R}_0 = 4.07$ and $\mathcal{R}_0 = 3.97$, respectively; we can see that the presence of one additional link in the ring increases the spectral radius of the transmission matrices and thus facilitates the spread of the disease.

We provide numerical simulations of the evolution of an epidemics for the different networks considered, showing the dynamics of the fraction of asymptomatic and symptomatic infected individuals (see Figures 4–7). In each simulations,

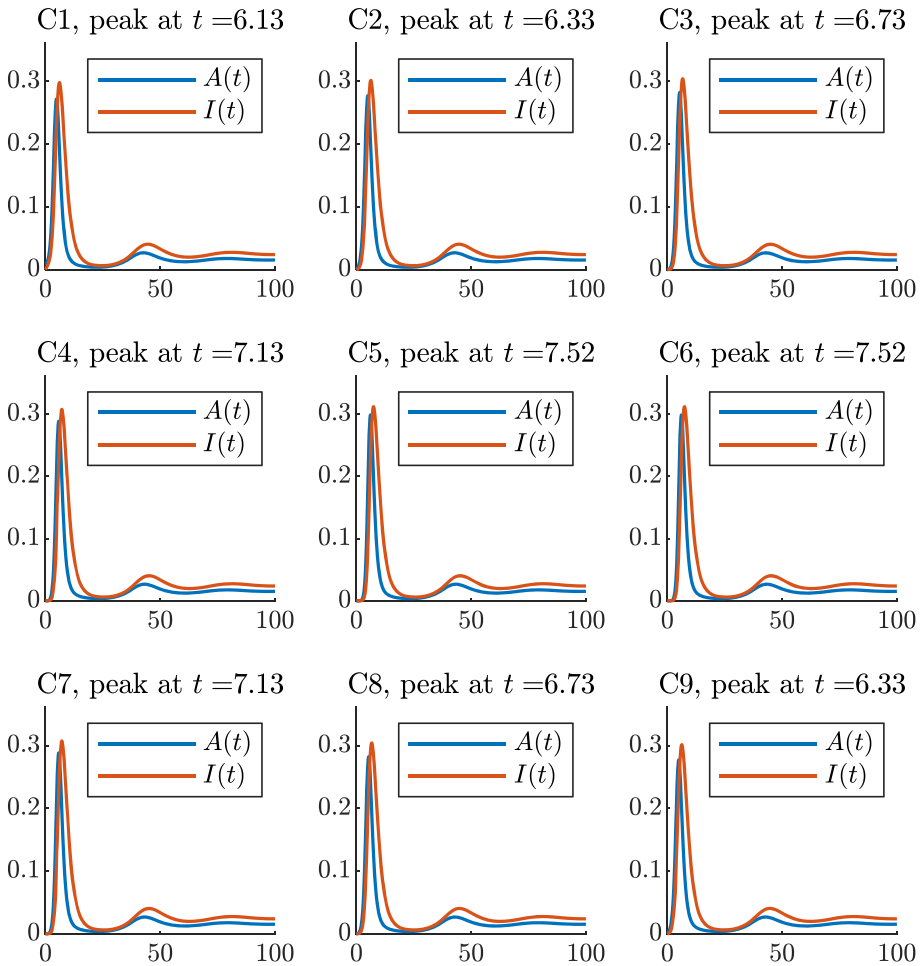

FIGURE 6 Evolution of the epidemic in each community of the ring network, see Figure 3C. The title of each subplot indicates the community it represents, as well as the peak time of infected individuals. In this setting, from (6), we obtain $\mathcal{R}_0 = 4.07$. Refer to Table 1 for the values of the parameters. [Colour figure can be viewed at wileyonlinelibrary.com]

in order to depict a realistic scenario, the epidemics starts in only one of the communities (Community 1), with a small asymptomatic fraction of the population and no symptomatic individuals, while the rest of the population is entirely susceptible. We obtain a delay in the start of the epidemics, directly proportional to the path distance of any community from Community 1: This is particularly visible in Figure 7. We observe a delay in the time of the peak, as well, although this is often less pronounced; this is clear in in Figure 6, in which communities with the same distance (path length) from Community 1 reach the peak at the same time. We underline that the time and the magnitude of the peak are directly proportional to the number of links of each community. Indeed, we can see that in the star network, the peak of the non-central communities happens exactly at the same time and has the same magnitude, as one would expect, see Figure 5. In the ring network (Figure 6), all the communities only have two links, thus the time and the magnitude of the peak are the same for communities at the same path distance from Community 1. In Figure 7, instead, the magnitude is the same for Communities 2–8 and is lower in Communities 1 and 9, which are less connected with the others. The peak is reached faster in Community 1, in which the epidemic starts, and occurs later in Community 9, since it is the further and the less connected of the network. We remark that this predictable behavior of the peak of infected individuals is due to the deterministic nature of the model, and thus of the numerical simulations.

For ease of interpretation, we plot the total number of asymptomatic infected individuals and symptomatic Infected individuals in all four cases; see Figure 8. The qualitative behavior of all simulations is the same: After a first spike, the dynamics converges towards the EE, through quickly damping oscillations. In all our simulations, the EE values of I are greater than the ones of A, as we expected from (17) and our choice of the parameters involved in the formula.

Notice the significantly lower peaks in Figure 8D, when compared to Figure 8C, even though the corresponding networks only differ for one edge, connecting Community 9 to Community 1, in which the epidemics start. Tables B1–B8

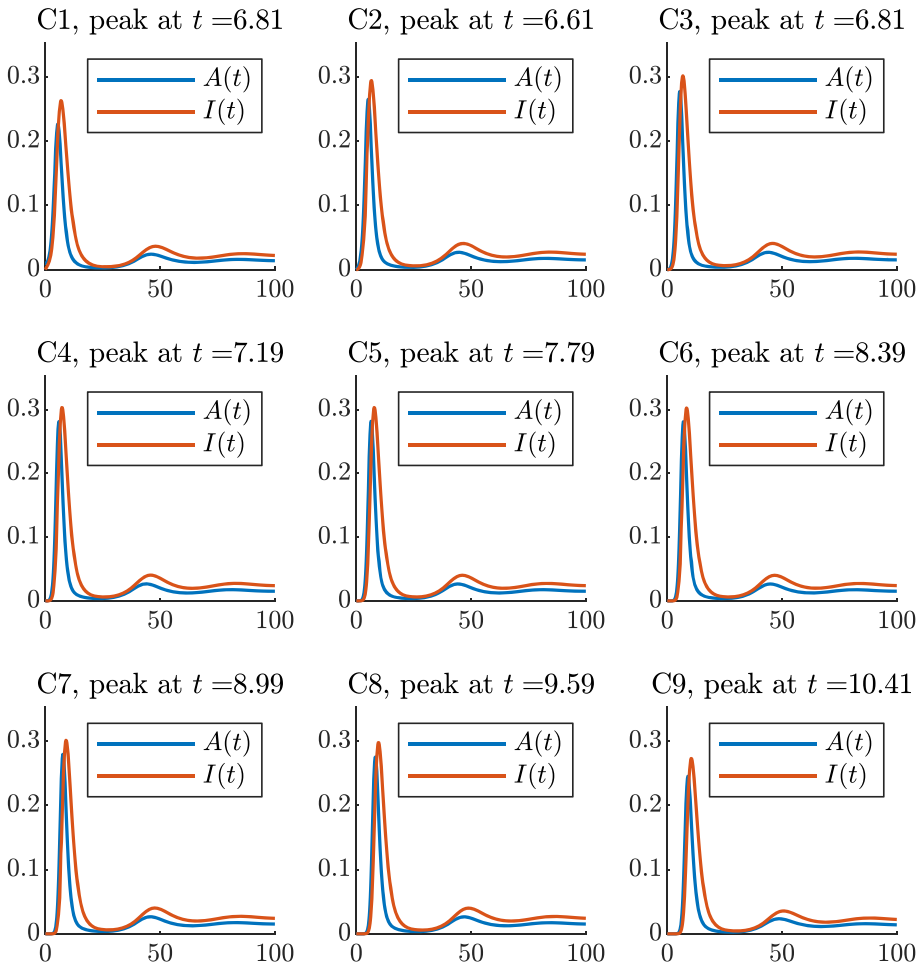

FIGURE 7 Evolution of the epidemic in each community of the line network, see Figure 3D. The title of each subplot indicates the community it represents, as well as the peak time of infected individuals. In this setting, from (6), we obtain $\mathcal{R}_0 = 3.97$. Refer to Table 1 for the values of the parameters. [Colour figure can be viewed at wileyonlinelibrary.com]

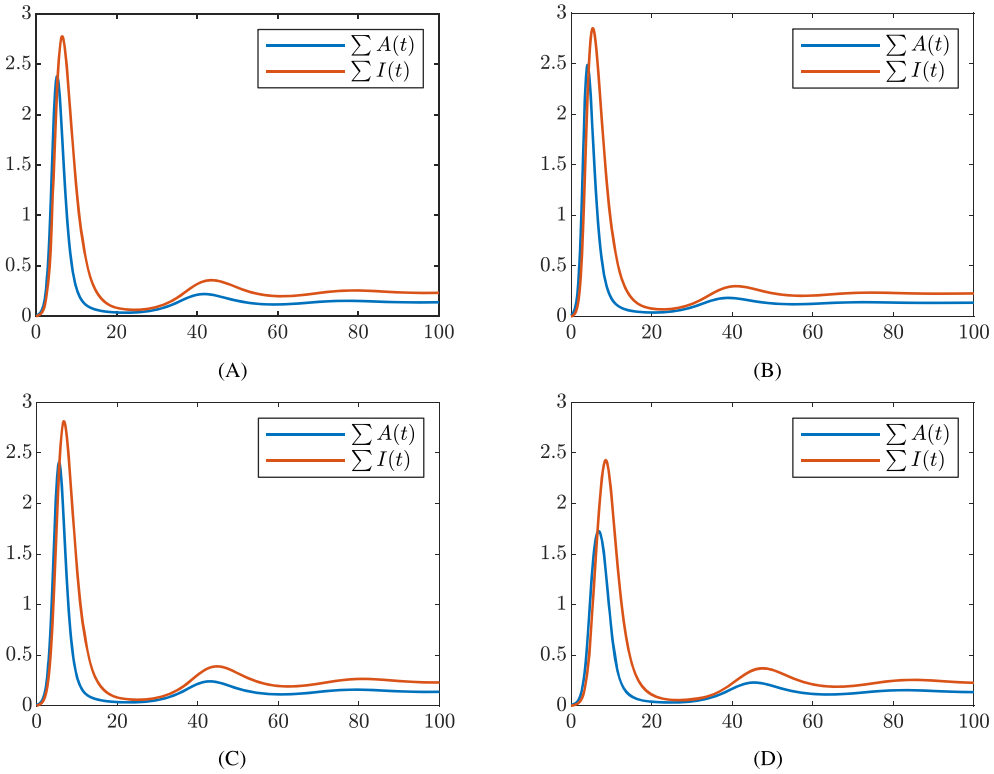

FIGURE 8 Total amount of Asymptomatic infected $\left(\sum A(t)\right)$ and symptomatic Infected $\left(\sum I(t)\right)$ in the four networks we simulate. Respectively, (A) cycle-tree network, see Figure 3A; (B) star network, see Figure 3B; (C) ring network, see Figure 3C; and (D) line network, see Figure 3D. The qualitative behavior is the same, that is, convergence towards the endemic equilibrium through damped oscillations. Refer to Table 1 for the values of the parameters. [Colour figure can be viewed at wileyonlinelibrary.com]

show the times in which the epidemic starts in each community, as well as the magnitude and the times of the peaks, both for asymptomatic (A) and symptomatic (I) infected individuals, for all the networks under investigations.

7 | CONCLUSION

We analyzed a multi-group SAIRS-type epidemic model with vaccination. In this model, susceptible individuals can be infected by both asymptomatic and symptomatic infectious individuals, belonging to their communities and to other adjacent communities.

We provided a stability analysis of the multi-group system under investigation; to the best of the authors' knowledge, this kind of analytical results was lacking in the literature. Precisely, we derived the expression of the basic reproduction number $\mathcal{R}_0$, which depends on the matrices which encode the transmission rates between and within communities. We showed that if $\mathcal{R}_0 < 1$, the DFE is GAS, that is, the disease will be eliminated in the long run, whereas if $\mathcal{R}_0 > 1$, it is unstable. Moreover, in the SAIRS model without vaccination ($v_i = 0$, for all $i = 1, \dots, n$), we were able to generalize the result on the global asymptotic stability of the DFE also in the case $\mathcal{R}_0 = 1$. We proved the existence of a unique EE if $\mathcal{R}_0 > 1$. We gave sufficient conditions for the local asymptotic stability of the EE; then, we investigated the global asymptotic stability of the EE in two cases. The first one regards the SAIR model (i.e., $\gamma = 0$) and does not requires any further conditions on the parameters besides $\mathcal{R}_0 > 1$.

The second is the case of the SAIRS model, with the restriction that asymptomatic and symptomatic individuals have the same mean recovery period, that is, $\delta_A = \delta_I$. In this case, we provided sufficient conditions for the GAS of the EE.

We leave as open problem the study of the global asymptotic stability of the EE for the SAIRS model with vaccination, in the case $\beta_A \neq \beta_I$ and $\delta_A \neq \delta_I$. Lastly, we conjecture that the conditions we derived to prove the asymptotic behavior of the model are sufficient but not necessary conditions, as our numerical exploration of various settings seems to indicate.

In this paper, we focused on a generalization of the SAIRS compartmental model proposed in Ottaviano et al. [16], by considering a network where each node represents a community; however, many others elements could be included in fur-

ther generalizations to increase realism. For example, we may consider a greater number of compartments, for example, including the "Exposed," "Hospitalized," or "Quarantined" groups, or consider a nonlinear incidence rate; one could also introduce an additional disease-induced mortality or an imperfect vaccination. We leave these as future research outlook.

ACKNOWLEDGEMENTS

The authors would like to thank Prof. Andrea Pugliese for the fruitful discussions, suggestions and careful reading of the paper draft. The research of Stefania Ottaviano was supported by the University of Trento in the frame "SBI-COVID - Squashing the business interruption curve while flattening pandemic curve" (Grant 40900013). Mattia Sensi and Sara Sottile were supported by the Italian Ministry for University and Research (MUR) through the PRIN 2020 project "Integrated Mathematical Approaches to Socio-Epidemiological Dynamics" (2020JLWP23). Open Access Funding provided by Politecnico di Torino within the CRUI-CARE Agreement.

CONFLICT OF INTEREST STATEMENT

This work does not have any conflicts of interest.

ORCID

Mattia Sensi https://orcid.org/0000-0002-6631-0242

REFERENCES

1. S. Bonaccorsi, S. Ottaviano, D. Mugnolo, and F. De Pellegrini, *Epidemic outbreaks in networks with equitable or almost-equitable partitions*, SIAM J. Appl. Math. **75** (2015), no. 6, 2421–2443.
2. S. Ottaviano, F. De Pellegrini, S. Bonaccorsi, D. Mugnolo, and P. Van Mieghem, Community networks with equitable partitions, *Multilevel strategic interaction game models for complex networks*, Springer Nature, Switzerland, 2019, pp. 111–129.
3. S. Ottaviano and S. Bonaccorsi, *Some aspects of the Markovian SIRS epidemic on networks and its mean-field approximation*, Math. Methods Appl. Sci. **44** (2021), no. 6, 4952–4971.
4. P. Van Mieghem, *The N-intertwined SIS epidemic network model*, Computing **93** (2011), no. 2-4, 147–169.
5. A. Lajmanovich and J. A. Yorke, *A deterministic model for gonorrhea in a nonhomogeneous population*, Math. Biosci. **28** (1976), no. 3, 221–236.
6. W. Huang, K. L. Cooke, and C. Castillo-Chavez, *Stability and bifurcation for a multiple-group model for the dynamics of HIV/AIDS transmission*, SIAM J. Appl. Math. **52** (1992), no. 3, 835–854.
7. J. Yu, D. Jiang, and N. Shi, *Global stability of two-group SIR model with random perturbation*, J. Math. Anal. Appl. **360** (2009), no. 1, 235–244.
8. H. R. Thieme, Local stability in epidemic models for heterogeneous populations, *Mathematics in biology and medicine*, Springer, Berlin, Heidelberg, 1985, pp. 185–189.
9. R. N. Mohapatra, D. Porchia, and Z. Shuai, *Compartmental disease models with heterogeneous populations: a survey*, Math. Anal. Appl. **143** (2015), 619.
10. H. Guo, M. Y. Li, and Z. Shuai, *Global stability of the endemic equilibrium of multigroup SIR epidemic models*, Canadian Appl. Math. Quart. **14** (2006), no. 3, 259–284.
11. H. Guo, M. Li, and Z. Shuai, *A graph-theoretic approach to the method of global Lyapunov functions*, Proc. Am. Math. Soc. **136** (2008), no. 8, 2793–2802.
12. M. Y. Li and Z. Shuai, *Global-stability problem for coupled systems of differential equations on networks*, J. Differ. Equat. **248** (2010), no. 1, 1–20.
13. Y. Muroya, Y. Enatsu, and T. Kuniya, *Global stability for a multi-group SIRS epidemic model with varying population sizes*, Nonlin. Anal.: Real World Appl. **14** (2013), no. 3, 1693–1704.
14. Y. Muroya and T. Kuniya, *Further stability analysis for a multi-group SIRS epidemic model with varying total population size*, Appl. Math. Lett. **38** (2014), 73–78.
15. D. Fan, P. Hao, D. Sun, and J. Wei, *Global stability of multi-group SEIRS epidemic models with vaccination*, Int. J. Biomath. **11** (2018), no. 1, 1850006.
16. S. Ottaviano, M. Sensi, and S. Sottile, *Global stability of SAIRS epidemic models*, Nonlin. Anal.: Real World Appl. **65** (2022), 103501.
17. M. Day, *Covid-19: identifying and isolating asymptomatic people helped eliminate virus in Italian village*, BMJ: British Med. J. (Online) **368** (2020), m1165.
18. D. P. Oran and E. J. Topol, *Prevalence of asymptomatic SARS-CoV-2 infection: a narrative review*, Ann. Internal Med. **173** (2020), no. 5, 362–367.
19. D. P. Oran and E. J. Topol, *The proportion of SARS-CoV-2 infections that are asymptomatic: a systematic review*, Ann. Internal Med. **174** (2021), no. 5, 655–662.

20. M. A. Johansson, T. M. Quandelacy, S. Kada, P. V. Prasad, M. Steele, J. T. Brooks, R. B. Slayton, M. Biggerstaff, and J. C. Butler, *SARS-CoV-2 transmission from people without COVID-19 symptoms*, JAMA Netw. Open **4** (2021), no. 1, e2035057.
21. D. Calvetti, A. P. Hoover, J. Rose, and E. Somersalo, *Metapopulation network models for understanding, predicting, and managing the coronavirus disease COVID-19*, Front. Phys. **8** (2020), 261.
22. M. Peirlinck, K. Linka, F. S. Costabal, J. Bhattacharya, E. Bendavid, J. P. A. Ioannidis, and E. Kuhl, *Visualizing the invisible: the effect of asymptomatic transmission on the outbreak dynamics of COVID-19*, Comput. Methods Appl. Mech. Eng. **372** (2020), 113410.
23. S. W. Park, D. M. Cornforth, J. Dushoff, and J. S Weitz, *The time scale of asymptomatic transmission affects estimates of epidemic potential in the COVID-19 outbreak*, Epidemics **31** (2020), 100392.
24. R. Li, S. Pei, B. Chen, Y. Song, T. Zhang, W. Yang, and J. Shaman, *Substantial undocumented infection facilitates the rapid dissemination of novel coronavirus (SARS-CoV-2)*, Science **368** (2020), no. 6490, 489–493.
25. L. Stella, A. P. Martínez, D. Bauso, and P. Colaneri, *The role of asymptomatic infections in the COVID-19 epidemic via complex networks and stability analysis*, SIAM J. Control Optim. **60** (2022), no. 2, S119–S144.
26. J. T. Kemper, *The effects of asymptomatic attacks on the spread of infectious disease: a deterministic model*, Bull. Math. Biol. **40** (1978), no. 6, 707–718.
27. E. J. Nelson, J. B. Harris, J. G. Morris, S. B. Calderwood, and A. Camilli, *Cholera transmission: the host, pathogen and bacteriophage dynamic*, Nat. Rev. Microbiol. **7** (2009), no. 10, 693–702.
28. N. I. Stilianakis, A. S. Perelson, and F. G. Hayden, *Emergence of drug resistance during an influenza epidemic: insights from a mathematical model*, J. Infect. Diseases **177** (1998), no. 4, 863–873.
29. M. Robinson and N. I. Stilianakis, *A model for the emergence of drug resistance in the presence of asymptomatic infections*, Math. Biosci. **243** (2013), no. 2, 163–177.
30. P. van den Driessche and J. Watmough, *Reproduction numbers and sub-threshold endemic equilibria for compartmental models of disease transmission*, Math. Biosci. **180** (2002), 29–48.
31. R. A. Horn and C. R. Johnson, *Matrix analysis*, Cambridge University Press, Cambridge, 2012.
32. P. van den Driessche and J. Watmough, Further notes on the basic reproduction number, *Mathematical epidemiology*, Springer, Berlin, Heidelberg, 2008, pp. 159–178.
33. Z. Shuai and P. van den Driessche, *Global Stability of infectious disease models using Lyapunov functions*, SIAM J. Appl. Math. **73** (2013), no. 4, 1513–1532.
34. H. W. Hethcote and H. R. Thieme, *Stability of the endemic equilibrium in epidemic models with subpopulations*, Math. Biosci. **75** (1985), no. 2, 205–227.
35. H. Shu, D. Fan, and J. Wei, *Global stability of multi-group SEIR epidemic models with distributed delays and nonlinear transmission*, Nonlin. Anal.: Real World Appl. **13** (2012), no. 4, 1581–1592.
36. M. Y. Li and Z. Shuai, *Global stability of an epidemic model in a patchy environment*, Canadian Appl. Math. Quart. **17** (2009), no. 1, 175–187.
37. S. Ruoyan and S. Junping, *Global stability of multigroup epidemic model with group mixing and nonlinear incidence rates*, Appl. Math. Comput. **218** (2011), no. 2, 280–286.
38. H. I. Freedman, S. Ruan, and M. Tang, *Uniform persistence and flows near a closed positively invariant set*, J. Dyn. Differ. Equat. **6** (1994), no. 4, 583–600.
39. M. Y. Li, J. R. Graef, L. Wang, and J. Karsai, *Global dynamics of a SEIR model with varying total population size*, Math. Biosci. **160** (1999), no. 2, 191–213.
40. J. P. La Salle, *The stability of dynamical systems*, SIAM, Philadelphia, 1976.
41. S. M. Moghadas and A. B. Gumel, *Global stability of a two-stage epidemic model with generalized non-linear incidence*, Math. Comput. Simul. **60** (2002), no. 1-2, 107–118.
42. N. Sherborne, K. B. Blyuss, and I. Z. Kiss, *Compact pairwise models for epidemics with multiple infectious stages on degree heterogeneous and clustered networks*, J. Theoret. Biol. **407** (2016), 387–400.
43. Y. Wang and J. Cao, *Global stability of a multiple infected compartments model for waterborne diseases*, Commun. Nonlin. Sci. Numer. Simul. **19** (2014), no. 10, 3753–3765.

How to cite this article: S. Ottaviano, M. Sensi, and S. Sottile, *Global stability of multi-group SAIRS epidemic models*, Math. Meth. Appl. Sci. **46** (2023), 14045–14071. DOI 10.1002/mma.9303

APPENDIX A

Proof of Claim 11. We recall that

$$\eta_i(z) = \frac{1}{\alpha + \mu_i + \delta_A}\left(z + \sum_{j=1}^{n} \beta_{ij}^{A}\left(A_j^* + h_j I_j^*\right)\left(1 + K_i^1(z) + K_i^2(z)\right)\right).$$

It is easy to see that if $\mathrm{Re}(z) \geq 0$, then $\mathrm{Re}(K_i^1(z)) > 0$. Now, we show that if $\mathrm{Re}(z) \geq 0$, then

$$\mathrm{Re}\left(1 + K_i^2(z)\right) = \mathrm{Re}\left(1 + \frac{1}{z + \mu_i + \nu_i + \gamma}\left((\delta_A - \nu_i) + \frac{(\delta_I - \nu_i)\alpha}{z + \delta_I + \nu_i}\right)\right) \geq 0. \tag{A1}$$

For ease of notation, we define

$$\varepsilon = (\delta_I - \nu_i)\alpha,\ h_1 = \mu_i + \nu_i + \gamma,\ h_2 = \delta_I + \nu_i,$$

and let $z = a + ib$ in (A1). If $\delta_A \geq \nu_i$, again, it is easy to see that if $\mathrm{Re}(z) \geq 0$, then

$$\mathrm{Re}\left(\frac{1}{z + h_1}(\delta_A - \nu_i)\right) \geq 0.$$

Now, let us show that

$$\mathrm{Re}\left(1 + \frac{\varepsilon}{(z + h_1)(z + h_2)}\right) \geq 0. \tag{A2}$$

We have that

$$\begin{aligned}
\mathrm{Re}\left(\frac{\varepsilon}{(z + h_1)(z + h_2)}\right) &= \mathrm{Re}\left(\frac{\varepsilon}{(a + h_1)(a + h_2) - b^2 + ib(2a + h_1 + h_2)}\right) \\
&= \mathrm{Re}\left(\varepsilon\frac{(a + h_1)(a + h_2) - b^2 - ib(2a + h_1 + h_2)}{((a + h_1)(a + h_2) - b^2)^2 + b^2(2a + h_1 + h_2)}\right) \\
&= \varepsilon\frac{(a + h_1)(a + h_2) - b^2}{((a + h_1)(a + h_2) - b^2)^2 + b^2(2a + h_1 + h_2)} \\
&= \varepsilon\frac{(P - b^2)}{(P - b^2)^2 + b^2S^2} = g(b),
\end{aligned} \tag{A3}$$

where we have introduced the notation

$$P = (a + h_1)(a + h_2) \text{ and } S = (2a + h_1 + h_2).$$

Since we assume $\delta_I \geq \nu_i$, we can see that the minimum of $g(b)$ is equal to

$$\frac{-\varepsilon}{2S\sqrt{P} + S^2},$$

and that

$$\begin{aligned}
\frac{-\varepsilon}{2S\sqrt{P} + S^2} &\geq \frac{-(\delta_I - \nu_i)\alpha}{2(2a + \mu_i + 2\nu_i + \gamma + \delta_I)\sqrt{((a + \mu_i + \nu_i + \gamma)(a + \delta_I + \nu_i))} + (2a + \mu_i + 2\nu_i + \gamma + \delta_I)^2} \\
&\geq \frac{-(\delta_I - \nu_i)\alpha}{2(\mu_i + 2\nu_i + \gamma + \delta_I)\sqrt{((\mu_i + \nu_i + \gamma)(\delta_I + \nu_i))} + (\mu_i + 2\nu_i + \gamma + \delta_I)^2} \\
&\geq -1.
\end{aligned}$$

The last inequality holds since by hypothesis

$$(\delta_I - \nu_i)\alpha \leq 2(\mu_i + 2\nu_i + \gamma + \delta_I)\sqrt{(\mu_i + \nu_i + \gamma)(\delta_I + \nu_i)} + (\mu_i + 2\nu_i + \gamma + \delta_I)^2,$$

thus, (A2) holds and the claim is proved.

APPENDIX B

In the following tables, we show the times in which the epidemic starts in each community, as well as the magnitude and the times of the peaks, both for asymptomatic (A) and symptomatic (I) infected individuals, for all the networks under

investigations. We consider an epidemic to have started in a community when the variable (either $I(t)$ or $A(t)$) exceeds the threshold value of 10^{-5}. We remark that the quantity I, meaning the fraction of symptomatic individuals, is the one which is more realistically and accurately tracked, in a real-world scenario.

TABLE B1 Values of the starting time of the epidemic and time and magnitude of the peak in each community for the cycle-tree network in Figure 3A for symptomatic infected I.

Community	Starting time of epidemic	Time of peak	Magnitude of peak
1	0	6.07	0.3011
2	0.006	6.07	0.3080
3	0.006	6.07	0.3291
4	0.1	6.75	0.3220
5	0.006	6.07	0.3268
6	0.65	7.64	0.2826
7	0.65	7.64	0.2826
8	0.17	7.10	0.2839
9	0.006	6.07	0.3077

Note: See also Figures 4 and 8A.

TABLE B2 Values of the starting time of the epidemic and time and magnitude of the peak in each community for the cycle-tree network in Figure 3A for asymptomatic infected A.

Community	Starting time of epidemic	Time of peak	Magnitude of peak
1	0	4.72	0.2773
2	0	4.72	0.2884
3	0.005	4.93	0.3222
4	0.12	5.33	0.3098
5	0.005	4.93	0.3188
6	0.4	6.24	0.2582
7	0.4	6.24	0.2582
8	0.2	5.54	0.2602
9	0	4.72	0.2878

Note: See also Figures 4 and 8A.

TABLE B3 Values of the starting time of the epidemic and time and magnitude of the peak in each community for the star network in Figure 3B for symptomatic infected I.

Community	Starting time of epidemic	Time of peak	Magnitude of peak
1	0	4.63	0.3581
2	0.08	5.64	0.2915
3	0.08	5.64	0.2915
4	0.08	5.64	0.2915
5	0.08	5.64	0.2915
6	0.08	5.64	0.2915
7	0.08	5.64	0.2915
8	0.08	5.64	0.2915
9	0.08	5.64	0.2915

Note: See also Figures 5 and 8B.

TABLE B4 Values of the starting time of the epidemic and time and magnitude of the peak in each community for the star network in Figure 3B for asymptomatic infected A.

Community	Starting time of epidemic	Time of peak	Magnitude of peak
1	0	3.48	0.3759
2	0	4.24	0.2727
3	0	4.24	0.2727
4	0	4.24	0.2727
5	0	4.24	0.2727
6	0	4.24	0.2727
7	0	4.24	0.2727
8	0	4.24	0.2727
9	0	4.24	0.2727

Note: See also Figures 5 and 8B.

TABLE B5 Values of the starting time of the epidemic and time and magnitude of the peak in each community for the ring network in Figure 3C for symptomatic infected I.

Community	Starting time of epidemic	Time of peak	Magnitude of peak
1	0	6.13	0.2981
2	0.01	6.33	0.3015
3	0.4	6.73	0.3041
4	0.5	7.13	0.3074
5	1.7	7.52	0.3117
6	1.7	7.52	0.3117
7	0.5	7.13	0.3074
8	0.4	6.73	0.3041
9	0.01	6.33	0.3015

Note: See also Figures 6 and 8C.

TABLE B6 Values of the starting time of the epidemic and time and magnitude of the peak in each community for the ring network in Figure 3C for asymptomatic infected A.

Community	Starting time of epidemic	Time of peak	Magnitude of peak
1	0	4.76	0.2718
2	0	4.95	0.2771
3	0.15	5.34	0.2822
4	0.27	5.72	0.2882
5	1.23	6.13	0.2985
6	1.23	6.13	0.2985
7	0.27	5.72	0.2882
8	0.15	5.34	0.2822
9	0	4.95	0.2771

Note: See also Figures 6 and 8C.

TABLE B7 Values of the starting time of the epidemic and time and magnitude of the peak in each community for the line network in Figure 3D for symptomatic infected I.

Community	Starting time of epidemic	Time of peak	Magnitude of peak
1	0	6.81	0.2629
2	0.02	6.61	0.2941
3	0.2	6.81	0.3015
4	0.81	7.19	0.3029
5	1.73	7.79	0.3031
6	1.88	8.39	0.3023
7	1.91	8.99	0.3011
8	2.03	9.59	0.2975
9	4.19	10.41	0.2728

Note: See also Figures 7 and 8D.

TABLE B8 Values of the starting time of the epidemic and time and magnitude of the peak in each community for the line network in Figure 3D for asymptomatic infected A.

Community	Starting time of epidemic	Time of peak	Magnitude of peak
1	0	5.40	0.2263
2	0	5.26	0.2650
3	0.08	5.54	0.2771
4	0.53	5.96	0.2811
5	1.26	6.42	0.2814
6	1.42	6.99	0.2807
7	1.57	7.58	0.2791
8	1.73	8.39	0.2751
9	3.64	8.99	0.2450

Note: See also Figures 7 and 8D.